THE EFFECT OF REPLICATED INTERMITTENT FASTING ON TYPE 2 DIABETIC AND NON-DISEASED HUMAN SKELETAL MUSCLE MYOBLASTS

A Thesis

By

LAEL K. CERIANI

BS, East Carolina University, 2018

Submitted in Partial Fulfillment of the Requirements for the Degree of

MASTER OF SCIENCE

in

BIOLOGY

Texas A&M University – Corpus Christi
Corpus Christi, TX

August 2020

August 2020

THE EFFECT OF REPLICATED INTERMITTENT FASTING ON TYPE 2 DIABETIC AND NON-DISEASED HUMAN SKELETAL MUSCLE MYOBLASTS

A Thesis

by

LAEL K. CERIANI

This thesis meets the standards for scope and quality of
Texas A&M University-Corpus Christi and is hereby approved.

Felix Omoruyi, PhD
Chair

Xavier Gonzales, PhD
Co-Chair

Jean Sparks, PhD
Committee Member

Daniel Newmire, PhD
Committee Member

August 2020

ABSTRACT

Fasting and intermittent fasting have become new fad diets that put the aging and diabetic populations at risk for muscle atrophy. Type 2 diabetes is associated with insufficient insulin secretion and affects millions of people globally. With doctors prescribing fasting diets to patients with the intention of fat loss, they could potentially be putting them at risk for enhanced muscle wasting. **PURPOSE:** The purpose of this study was to examine the effects of nutrient stress on human skeletal muscle metabolism, with an emphasis on oxidative stress and atrophy markers in healthy and diabetic cell models. **METHODS:** Human skeletal muscle myoblast cells (HSMM) and diabetic human skeletal muscle myoblast cells (D-HSMM) were cultured in a 37° C and 5% CO2 incubator. At 80-90% confluency,10^5 cells were transferred into four 24 well plates and were incubated for 48h with standard culture media. The cells were then incubated for 12 or 24 hours with media containing varying serum concentrations: 5%, 10%, and 15%. The media contained either fetal bovine serum (FBS) or pooled human serum (HS) from healthy and diabetic patients (Doctors Regional, Corpus Christi TX). Following the 24 hours, cell viability and density were determined, and sandwich enzyme linked immunosorbent assay kits were performed to measure the amount of SOD1, Atrogin-1, and TNF-α in serum. TaqMan gene array plates were used to qualitatively assess gene expression in several atrophy biomarkers through RT-PCR reaction assessed through Quant Studio 3. **RESULTS:** Gene expression revealed 1.187-fold change in Myostatin and a 1.378-fold change in AKT_2 in 15% D-HSMM model. A 0.081-fold change was seen in Atrogin-1 in the 5% D-HSMM model. HS models in HSMM and D-HSMM cells show significant impact of treatment concentration on SOD1 expression ($p<0.0001$). The TNF-α ELISA suggests that time has a significant effect on TNF-α

concentration for HSMM cells plated with FBS (p=0.0211). Treatment concentration in HSMM HS model revealed a significant effect of treatment concentration (p=0.0116). An Atrogin-1 ELISA revealed virtually no presence in serum. **CONCLUSION:** The results indicate that the different nutrient states have deleterious effects on muscle cells through oxidative stress and inflammation. Upregulation in atrophy biomarkers also indicate instances of muscle wasting. The promotion of nutrient deprivation or fasting should be done with caution to avoid harmful outcomes in healthy and disease states.

Key Words: Fasting, Intermittent Fasting, Skeletal Muscle, Muscle Atrophy, Type 2 Diabetes, Nutrition

DEDICATION

This work is dedicated to my mother, Dylann Ceriani. Her intelligence, work ethic, and passion for knowledge are all I wish to be. I am very lucky to have such a great role model. Without her constant support and unyielding love this work (and my entire being) would not be possible.

ACKNOWLEDGEMENTS

This work is amalgamation of thoughtful advice and encouragement from the many people who have helped me and mentored me throughout this process. I would first like to acknowledge my thesis advisor and co-chair, Dr. Felix Omoruyi. I am deeply grateful for the opportunity to be accepted as his graduate student and for his guidance and encouragement. I have learned to be a better researcher because of lessons he has taught me. Secondly, I would like to thank my co-chair Dr. Xavier Gonzales. His patience and understanding are values I truly wish to emulate. I am very thankful for his guidance and the time he took out of his very busy schedule to guide me through this journey. His expertise was very valuable and was relied upon throughout this project. I would also like to thank Dr. Jean Sparks, for her excellent problem-solving skills, patience, and her uncanny ability to calm any anxieties that I had. I would also like to acknowledge my committee member Dr. Daniel Newmire, who offered valuable insight into this project and offered much needed encouragement. His persistence and dedication to me is one of the main reasons this project was completed. Lastly, I would like to thank my fellow graduate students, Louay Bachank and Jeanette Lindstrom, as well as several undergraduate students, for always being there when I needed help running experiments, and when they offered much needed advice. They made this journey not only possible, but enjoyable.

This project was supported through the Hispanic Serving Institutions Education [grant no. 2016-38422-25543/project accession no. 1009881] from the USDA National Institute of Food and Agriculture. Any opinions, findings, conclusions, or recommendations expressed in this

work are those of the authors and do not necessarily reflect the view of the U.S. Department of Agriculture.

TABLE OF CONTENTS

CONTENTS PAGE

LIST OF FIGURES

FIGURE PAGE

LIST OF TABLES

TABLE PAGE

1. INTRODUCTION

1.1 FASTING

Periods of voluntary abstinence from food or drink has been practiced for millennia in many cultures. The Paleolithic era was one of hunter-gatherers characterized by periods of feasting followed by long periods of fasting. There are also several religious traditions that call for an extended fast, which have been practiced for thousands of years[1]. While fasting is not a new concept, intermittent fasting has become increasingly popular, especially in the fitness and weight loss communities. Intermittent fasting (IF) is an eating style where one eats within a specific block of time and fasts the remainder of the time (i.e. 16-48 h). There are many blogs and articles full of anecdotal evidence of its effectiveness, and it has been speculated that it can promote weight loss, lower blood pressure and cholesterol, increase insulin sensitivity, and reduce the risk of cancer. Through the study of many different model organisms, researchers have discovered that certain regulatory pathways are highly conserved to help maintain health in times of energy scarcity. There are several fasting studies that focus on the metabolic effects of yeasts, bacteria, nematodes, and rodents[2–4], which demonstrate the positive correlation to fasting and longevity and disease prevention. Nutrient depletion has been shown to activate autophagy (self-eating), a process by which the cell degrades nonfunctional proteins and oxidizes free fatty acids[5]. Autophagy has been linked to weight-loss, but this might be connected to enhanced muscle wasting[6]. In many clinics, physicians are prescribing treatments of water only or low calorie (fewer than 200 kcal/day) fasting regimens. These fasts can last 1 week or longer, with the intention of weight management and disease prevention or treatment[1]. While there are reported benefits of fasting, the line between effective and destructive is still unclear. Research suggests that fasting is the most potent non-genetic autophagy stimulator[7], although the effects

these have on different organ systems has not been fully elucidated. Autophagy has shown a paradoxical effect in cancer cells and is context dependent[8]. The dysregulation of autophagy leads to several cancer signaling pathways that are involved with both tumor suppression[9,10] and oncogenesis[10]. There are several studies with conflicting evidence, and further research is necessary.

It is also important to contextualize fasting diets regarding human models. While there are reported benefits in non-human fasting studies, there are several other ethical and practical factors that must be considered in the human model. The sustainability of an IF diet in humans is questionable due to hunger pains, which were not shown to habituate during fasting periods in a study observing nonobese subjects[11]. Mood swings, eating disorders, and other factors are also indicators of unhealthy outcomes seen in fasting diets[12]. Reported human studies [11,13–15] have shown varying results, and further research needs to be conducted. With limited research on IF, and even fewer human clinical trial studies, it is imperative to determine the effects such a fast may have. A rodent study suggests that the decline in muscle mass that occurs during the normal aging process of mice is prevented by 40% in calorie restricted and intermittent fasted rats. However, it is unknown what this effect will be in humans, especially for aging and diseased individuals. This study aims to further elucidate the effect of a simulated fast on human skeletal muscle cell lines regarding specific atrophy and stress markers.

1.2 MUSCLE WASTING

There are two highly conserved pathways implicated in atrophying skeletal muscle. The proteolytic mechanisms involved with muscle wasting are ubiquitin-proteasome and autophagy-lysosomal systems. In ubiquitin proteasome systems, ubiquitin is attached and conjugated to target proteins via E1, E2, and E3 enzymes. Once tagged, they are degraded through a

proteasome[16]. In the autophagic/lysosomal system, portions of cells are sequestered via an autophagosome which is then fused with a lysosome, where the content is then digested via acid hydrolysis[17]. While the molecular mechanisms of these systems are well known, the regulatory systems and networks need to be further defined.

Skeletal muscle tissue is pliable and can respond to anabolic or catabolic stimuli. Anabolic stimuli including insulin and insulin growth factor 1 (IGF-1) lead to muscle protein synthesis, while catabolic stimuli like inflammation and energy imbalance lead to protein breakdown and degradation[6]. Decreased nutrient availability can lead to an upregulation in catabolic pathways and activation of Forkhead box O (FOXO) transcription factors. This group of proteins is subgroup O of the Forkhead box family. There are four classes of FOXO: FOXO1, FOXO3, FOXO4, and FOXO6[18]. The FOXO class have the characteristic of being regulated by the insulin/PI3K/Akt signaling pathway[19]. In a normal unstressed state, the insulin/PI3K/Akt pathway suppresses the expression of ubiquitin ligase muscle atrophy F-box 32 (FBXO32/Atrogin-1/MAFbx) by inactivating FOXO transcription factors. Protein kinase B (Akt) is stimulated by insulin and insulin growth factor 1 (IGF-1) which then activates mammalian target of rapamycin (mTOR) which leads to muscle protein synthesis. In a fasted state, Akt and its subsequent downstream targets are decreased. This allows FOXO expression to occur. Specifically, FOXO3 acts on the Atrogin-1 promoter to induce Atrogin-1 transcription. This ubiquitin ligase causes dramatic atrophy of muscle fibers and myotubes[20]. Appropriately, when Atrogin-1 is knocked down in murine models, it prevents muscle loss during fasting[21]. Relatedly, in myotubes when FOXO3 activation is blocked by a dominant-negative construct, Atrogin-1 induction by starvation is prevented[20]. Studies have also shown that upregulation of ubiquitin proteasomal pathways due to nutrient stress may lead to an elevated degradation of lean muscle

mass[22]. Likewise, downstream regulators of FOXO, Atrogin-1 and Muscle ring finger 1 (MuRF-1) have shown to be strongly induced atrophy genes[23,24].

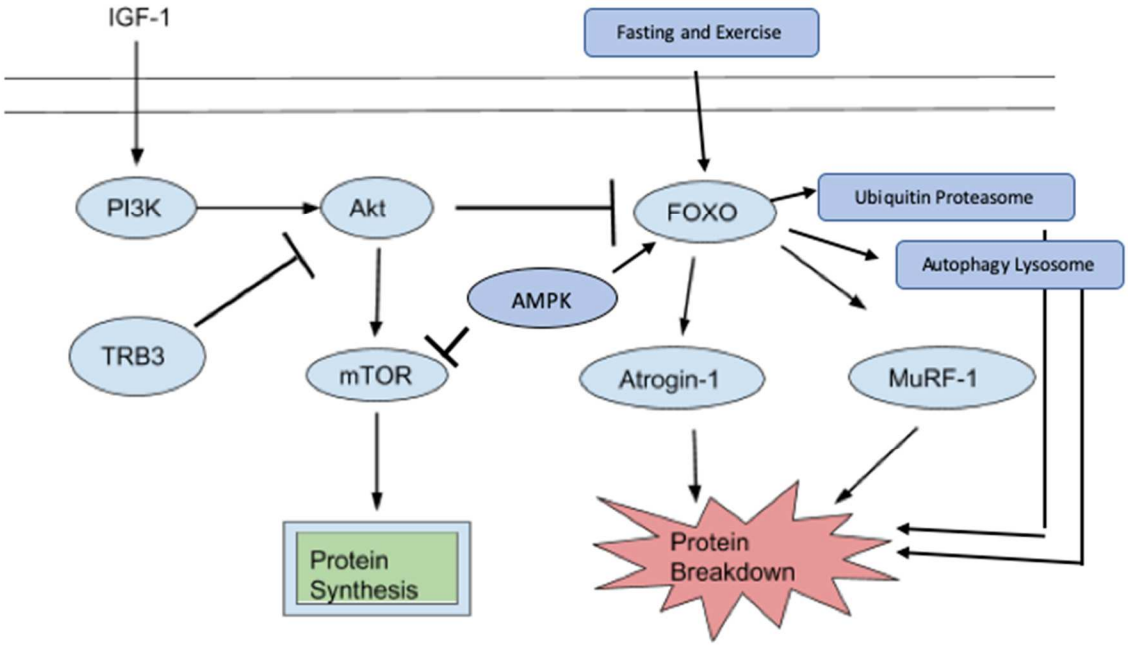

Figure 1: Simplified IGF/PI3K/Akt muscle protein signaling pathway

Along with the ubiquitin proteasomal pathway, the autophagy-lysosomal system has been shown to upregulate during fasting. Autophagy causes the bulk degradation of proteins and organelles by lysosomal enzymes. Interestingly, the FOXO3 transcription factor induces autophagy *in vivo*[25]. This serves as further evidence that FOXO transcription factors play a critical role in proteolysis, as FOXO3 regulates the two major systems of protein breakdown in skeletal muscle.

Also, in a fasting related autophagic response in rats, notable plantaris muscle loss was observed[22]. Ultimately, the risk of a prolonged fast is death by starvation. This outcome is often caused by muscle degeneration of the heart and its eventual failure[26]. While this only occurs in

extreme starvation, the impacts of intermittent fasting on muscle wasting are currently debated in literature.

1.3 DIABETES AND OXIDATIVE STRESS

Diabetes mellitus (diabetes) is a group of chronic metabolic syndromes characterized by elevated blood glucose levels with biochemical alterations in carbohydrate and lipid metabolism. There are three major types: type 1, type 2, and gestational diabetes. Type 1 diabetes (T1D) is associated with the deficiency or absence of insulin production by the beta cells of the pancreas. Type 2 diabetes, the most common form of diabetes (90-95% of diagnoses), is marked by decreased insulin sensitivity (insulin resistance) or a defect in insulin secretion. Gestational diabetes occurs during pregnancy and displays insulin resistance similar to T2D. This insulin resistance is thought to occur due to increased pregnancy hormones interfering with the insulin receptor. Insulin regulation returns to normal after delivery when hormones return to normal levels[27]. Inability to receive glucose in skeletal muscle due to insulin resistance in T2D results in oxidative stress and increased muscle atrophy[28]. Oxidative stress is caused by an excess of reactive oxygen species (ROS), which are free radicals that are continuously generated as products of oxidative metabolism. Oxidative stress can lead to damaged DNA, proteins, and other cellular components causing cell death[29]. Oxidative stress increases within a cell because of decreased antioxidant activity, which is seen in many diseases including T2D[26].

Oxidative stress is closely linked to impaired metabolic homeostasis and increased inflammation, which plays a significant role in the development of insulin resistance seen in T2D[28]. Several biomarkers of oxidative stress and inflammation have been utilized in previous research[30,31] to study the effects of insulin resistance in T2D. Inflammation and atrophy biomarkers secreted by muscle cells include IL-6[32,33] and TNF-alpha[34]. Elevated levels of these

cytokines indicate inflammation and potential atrophy and serve as good biomarkers of metabolic dysregulation in skeletal muscle.

Oxidative stress biomarkers include catalase (CAT) and superoxide dismutase (SOD). Superoxide is a harmful ROS primarily produced by oxygen metabolism. SOD is an antioxidant enzyme that converts superoxide into molecular oxygen and hydrogen peroxide, which are less toxic compounds. Catalase converts harmful hydrogen peroxide into water and oxygen, acting as an effective neutralizer. It is the main regulator of hydrogen peroxide. In the case of CAT deficiency there is excessive ROS and subsequent oxidative stress; causing damage and insulin resistance[26] by disrupting various points in insulin receptor signal transduction, ultimately resulting in decreased expression of the GLUT4 transporter in the cell membrane[28]. Chronic exposure to hyperglycemia has also been shown to increase the production of hydrogen peroxide and downregulate gene expression of CAT[32].

1.4 INFLAMMATION

Myokines are peptides or proteins that are released from skeletal muscle that exert autocrine, paracrine, and endocrine effects[35]. Inter-organ crosstalk mediated by myokines is important to characterize, especially in states of metabolic dysregulation. Contracting muscle has shown to release certain myokines that create cross-talk to visceral fat which is why physical inactivity can lead to weight gain and metabolic issues[36]. In patients that display one or more characteristics of metabolic syndrome, characterizing these myokines and their functions can lead to advancement in therapeutic strategies. Inflammation is a common risk factor with diabetes. Chronic inflammation has been shown to cause insulin resistance[37,38] and is caused by several proinflammatory mediators. In muscle, there are several expressed myokines, including Interleukin-6 (IL-6), Interleukin-8 (IL-8), Interleukin-15 (IL-15), Brain-derived neurotrophic

factor (BDNF), Leukemia inhibitory factor (LIF), Fibroblast growth factor 21 (FGF21), and Follistatin-like-1 and Tumor necrosis factor alpha (TNF-α), among others[39]. Most notable, TNF-α is a known pro-inflammatory and has been shown to decrease protein synthesis especially in fast twitch muscle[40]. IL-6 is widely known as the first discovered myokine, and has been shown to produce both pro and anti-inflammatory effects that are context dependent, reviewed by Pederson et al[39]. Inflammaging (chronically inflamed)[41] muscle poses many risk factors to disease, including diabetes.

1.5 SERUM STARVATION

Although there are currently several serum starvation studies, a standardized protocol has yet to be defined. The act of serum starvation can denote several types of removal of partial or all serum in media. It has been called serum deprivation, depletion, removal, and withdrawal, among others. All of these strategies employ different protocols, and some just state that the cells were starved with little elaboration. While these problems have been addressed[41], there is still need for standardization. Cellular starvation has been used to test metabolic and molecular biological pathways and has proven to be an efficient and useful technique.

Some studies claim that starving cells prepares them for an experiment in serum free conditions, and is not regarded as the official experiment[42,43]. Serum, typically bovine or horse derived, is a complex undefined medium and its contents can confound experiments based on varying composition. Because of this, some find it advantageous to starve cells by removing these unknown variables[44]. Others have found that serum deprivation causes disruptions in cell proliferation and leads to increases in cell death[45]. This in turn causes intracellular proteins being passively released, which significantly affects results and the pattern of expressed proteins[45]. This topic is currently debated in literature, but it is clear that many factors play a role in the

outcome regarding serum starvation. For example, serum starvation produces cell type and time dependent effects[41] Pirkmajer and Chibalin (2011) reported that human myotubes respond to serum starvation with a pronounced increase in ERK1/2 phosphorylation, while in rat L6 myoblasts it appears to downregulate[41]. Serum shock (50% serum) has also been utilized in certain cell culture models to elicit a desired effect. Of the many factors that play a role in serum starvation, the type of serum is important as well. It has been reported that mesenchymal stem cells proliferate more in the presence of human serum than FBS[46]. Some theorize that human cells might potentially prosper in the presence of hormones and growth factors intrinsic to humans, although the precise underlying mechanisms are unknown.

1.6. PURPOSE

The purpose of this study was to assess the effect of replicating an intermittent fast (nutrient deprivation) on oxidative markers, inflammatory markers, and gene expression in Type 2-diabetic and non-diseased, human skeletal muscle myoblast cells. This study also assessed the effects of overnutrition (nutrient excess) in these cell lines.

2. OBJECTIVES

Objective 1 aims to determine the impact of nutritional stress (both fasted and nutrient excess models) in HSMM and D-HSMM cells exposed to 15%, 10%, and 5% fetal bovine serum (FBS) supplemented growth media for 12 and 24 hours. This objective also aims to elucidate the effect of nutritional concentrations on biomarkers of muscle inflammation, oxidative stress, and protein degradation/synthesis. It was hypothesized that the nutrient stress (in both models) would cause an increase in proteolytic, oxidative, and inflammatory biomarkers as well as decreased cell viability.

Objective 2 aims to determine the impact of nutritional stress (both fasted and nutrient excess models) in HSMM and D-HSMM cells exposed to 15%, 10%, and 5% pooled human serum (HS) supplemented growth media for 12 and 24 hours. The nutritional differences from HS to FBS will be evaluated. The objective aims to compare the efficacy of FBS compared to human serum in human skeletal muscle cell culture. Utilizing human serum compared to FBS reflects systemic conditions to that of an *in vivo* model and may be more physiologically relevant to human models[47]. Similar to objective 1, this objective also aims to determine the effect of nutritional stress concentrations on biomarkers of muscle inflammation, oxidative stress, and protein degradation/synthesis. It was hypothesized that nutrient deprivation and excess treatment would depict and increase in proteolytic, oxidative, and inflammatory biomarkers along with decreased cell viability.

	Non-diseased (HSMM)	**Type 2 Diabetic (D-HSMM)**
Objective 1 (Standard growth media)	12 hr. 5%, 10%, 15% FBS	12 hr. 5%, 10%, 15% FBS
	24 hr. 5%, 10%, 15% FBS	24 hr. 5%, 10%, 15% FBS
Objective 2 (Human derived growth media)	12 hr. 5%, 10%, 15% HS	12 hr. 5%, 10%, 15% DHS
	24 hr. 5%, 10%, 15% HS	24 hr. 5%, 10%, 15% DHS

Table 1: Schematic of Objectives. FBS denotes fetal bovine serum supplemented media, HS denotes healthy human serum supplemented media, and DHS denotes diabetic human serum supplemented media.

3. MATERIALS AND METHODS

3.1 SKELETAL MUSCLE CELL LINE DEMOGRAPHICS

Type 2 diabetic and non-diseased human skeletal muscle myoblasts were purchased from Lonza Inc, Walkersville, MD USA (referred to as D-HSMM and HSMM, respectively). Lonza reports that after informed and legal consent, the cells were isolated from donated human tissue. The D-

HSMM cell line was donated from a 68-year-old Caucasian male, while the HSMM cell line was donated from a 38-year-old Caucasian male. Further characteristics can be found in table 2.

	HSMM	**D-HSMM**
Donor Age (years)	38	68
Donor Race	Caucasian	Caucasian
Donor Sex	Male	Male
Donor BMI	26	--
Virus Testing	Not detected	Not detected
Microbial Testing	Negative	Negative
Cell Performance: Viability	91%	93%

Table 2: Skeletal Muscle Cell Line Characteristics

3.2 SAMPLE AND MEDIA PREPARATION

Human skeletal muscle myoblast and diabetic human skeletal muscle myoblast cells (Lonza Inc., Walkersville, MD) were cultured in falcon flasks with skeletal muscle growth media-2 (SkGM-2 medium) containing Fetal Bovine Serum (FBS), human epidermal growth factor (HEGF), dexamethasone, L-Glutamine, 30mg/ml Gentamycin, 15 µg/ml Amphotericin, 50 U/mL penicillin, and 50 mg/mL streptomycin. Cells were incubated at 37°C in a humidified incubator containing 5% CO_2. After 24 hours, cells adhered to the bottom of the flask. Media was changed approximately every 48-72 hours. When cells reached confluency (~10^6 cells/mL), cells were harvested with trypsin according to manufacturer's instructions (Lonza Inc., Walkersville, MD).

Experimental media was prepared by decreasing or increasing the concentration of serum in standard culture media. Lonza protocol calls for typical culture media to be 10% FBS. The experimental media either contained 15%, 10%, 5%, or 0% serum. Other media components were not diluted and were kept at manufacturers protocol with the exception of one experimental media containing no dexamethasone and 10% serum. Different types of serum were also utilized during experimentation. Media contained varying concentrations of either FBS (Lonza Inc., Walkersville, MD) or pooled human serum from healthy or diabetic patients (Doctors Regional Hospital, Corpus Christi, TX). Normal human serum was defined as having a blood glucose levels less than 105 mg/dL and diabetic serum was defined as having a blood glucose level greater than 200 mg/dL. Comprehensive metabolic panel and lipid panels were also performed on both non-diabetic and diabetic human serum, shown in table 3 and 4.

Component	Non-Diabetic (HS) Value (non-fasted)	Type 2 Diabetic (DHS) Value (non-fasted)
Glucose (mg/dL)	105	206
BUN (mg/dL)	14	20
Creatinine (mg/dL)	0.83	1.13
Sodium (mmol/L)	141	140
Potassium (mmol/L)	4.1	4.1
Chloride (mmol/L)	106	105
Carbon Dioxide (mmol/L)	23	20
Calcium (mg/dL)	9.0	8.7
Total Protein (gm/dL)	6.4	6.3
Albumin (g/dL)	3.5	3.1
Bilirubin, Total (mg/dL)	0.7	0.5
AST (u/L)	52	71
ALT (u/L)	55	73
Alkaline Phosphatase (u/L)	89	138
Calculated Osmo	293	299
Anion Gap	12	15
Insulin (mIU/mL)	12.9	15.1
T4, Free (ng/dL)	1.2	1.3
T4, Total (ug/dL)	8.5	8.8
TSH (uIU/mL)	2.22	1.96
Anti-Thyroglobulin (uIU/mL)	24	22
Anti-Thyroid Peroxidase (U/mL)	45.8	33.2

Vitamin D, 25 Hydroxy (ng/mL)	23.1	20.1

Table 3: Comprehensive Metabolic Panel

Component	Non-Diabetic (HS) Value (non-fasted)	Type 2 Diabetic (DHS) Value (non-fasted)
Cholesterol (mg/dL)	160	151
HDL (mg/dL)	42	37
Triglycerides (mg/dL)	158	152
LDL, calculated (mg/dL)	86	84
VLDL, calculated (mg/dL)	32	30

Table 4: Lipid Panel

Two batches of human serum were pooled from patients at Doctors Regional Hospital in Corpus Christi, Texas. The first group was obtained from non-diabetic individuals. The blood glucose level for healthy serum was 105 mg/dL, slightly above levels typically seen in non-diabetic individuals. We were unable to ensure that all individuals had been fasting at the time of blood draw, so elevated levels may be reflected. The second group was collected from diagnosed type-two diabetic patients.

3.3 DETERMINATION OF CELL CONCENTRATION AND VIABILITY

Cell viability and concentration was determined via hemocytometer. A 1:1 ratio of 100 µL 0.4% trypan blue and cell suspension were vortexed in a 0.5 mL centrifuge tube. The dilution factor used was 2. Of this 200 µl trypan blue and cell suspension solution, 10 µL were pipetted into the hemocytometer chamber and covered with a glass coverslip. Of the 9 total one-millimeter squares on the grid, the four corners and center squares were counted. Shown in figure 2. Cell counts were determined using a factor 10^4, taking into account that each square has a volume of 0.0001 mL (1mm x 1mm x 0.1mm = 0.1 mm^3). Viable cells remained transparent while non-viable cells were stained blue.

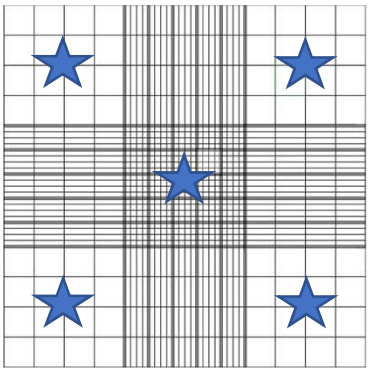

Figure 2: Hemocytometer Grid: Stars indicate hemocytometer gridlines that were counted out of the 9 total squares

A 10% positive control was also recorded. Along with the varying levels of serum, different types of serum were also recorded. Cells were plated with standard protocol FBS and were also plated from pooled human serum from healthy and diabetic patients. One hundred thousand cells were plated and were incubated in standard media for 48 hours to allow for plate adherence and growth to ~10^6 cells/mL. Cell densities and viabilities were recorded after exposing HSMM and D-HSMM cells to varying serum types and concentrations after 12 and 24 hours. Cell density was measured as number of cells present per mL of media. Cell viability was measured as number of live cells divided by the total number of cells (alive + dead) multiplied by 100.

Cell viability was determined by the following formula:

Percent viable = number of viable cells / numbers of total cells counted x 100

The total number of cells per unit volume was determined by the following formula:

Cells/mL = average viable cells counted / number of squares counted x dilution factor x 10^4

3.4 EXPERIMENTAL DESIGN

3.4.1 CELL PLATING

Initially, 10^5 cells were plated in each well of four 24-well polystyrene non-pyrogenic cell culture plates. The plated cells were incubated at 37° C and 5% CO_2 for 48 hours with SkGM-2

Medium. At the conclusion of the 48-hour incubation, cells had adhered to the bottom of the wells. The standard culture media was removed and discarded, and the experimental media was placed in the appropriate wells. In the human serum samples, HSMM cells were plated with the pooled normal serum and D-HSMM cells were plated with the diabetic serum.

3.4.2 NUTRIENT DEPLETION AND EXCESS MODEL

There are several serum starvation models, but there are very few employed in human muscle myoblasts. To our knowledge, a starvation model has been done in C2C12 mouse myoblast cells[48] but none on diseased human skeletal muscle myoblasts with the intention of observing atrogenes, oxidative markers, and inflammation markers.

This is a novel model, while employing aspects and protocols from other serum starvation experiments in other cell lines[41]. Both HSMM and D-HSMM cells were plated with 5%, 10%, and 15% FBS or HS. As a negative control, HSMM cells were plated with 0% serum. The presence or absence of dexamethasone, a synthetic steroid, was also considered when designing this experiment. Dexamethasone is a glucocorticoid and is typically utilized as a negative regulator of muscle mass. Lonza Inc, as well as many other companies, include small amounts (0.5mL Dexamethasone/500mL media) of dexamethasone in the standard cell culture media to inhibit the differentiation of myoblasts into myotubes, and mitigate inflammation. The effects of dexamethasone were shown to have varying effects at differentiation points[49]. Media with no dexamethasone was prepared and was evaluated at 10% FBS and HS in HSMM cells. It is also important to note that when cells were plated with human serum, the HSMM cells were plated with non-diseased serum, and D-HSMM cells were plated with T2D serum. The most notable difference in these two serums is the blood glucose levels, however there were other

confounding factors present, like the presence or absence of certain hormones that were not measured.

3.5 BIOMARKER ANALYSIS

3.5.1 ENZYME LINKEDIMMUNOSORBENT ASSAY

Sandwich Enzyme linked immunosorbent assays (ELISA) were used to analyze inflammation marker Tumor Necrosis Factor Alpha (TNF-α), oxidative stress marker Superoxide Dismutase 1 (SOD-1), and atrophy marker F-Box protein 32 (Atrogin-1) by capture of and quantification of antigens (Ray Biotech, Norcross, GA and MyBioSource San Diego, CA). Frozen and refrigerated reagents were brought to room temperature before use. A prepared standard (specific to the target protein) along with samples were added to a 96-well plate and were incubated for 2.5 hours at room temperature. The solution was then decanted and discarded. The plate was washed with wash buffer 4 times manually with a squirt wash bottle. One hundred µL of prepared biotinylated antibody was added to the wells. The plate was covered and incubated for 1 hour and then was decanted off, discarded, and washed as before. Following the wash, 100 µL of prepared streptavidin solution was added to each well. The plate was covered and incubated at room temperature for 45 minutes. The solution was then be decanted, discarded and washed as before. Following the wash, 100 µL of chromogenic substrate was added to each well, and the plate was developed at room temperature (in the dark) for 30 minutes. After 30 minutes, 50 µL of stop solution was added to each well, and the solution changed from blue to yellow. The plate was evaluated within 30 minutes with absorbances read at 450 nm on a spectrophotometer (BioRad Laboratories, Hercules, CA), and concentration of target protein was calculated from the standard curve.

Oxidative stress was measured through the concentration of superoxide dismutase 1 (SOD1) found in sandwich ELISAs when compared with a standard curve. By measuring the amount of SOD1 in each sample, we were able to examine the relative amount of oxidative stress for each serum concentration and make connections to muscle atrophy. Inflammation was measured through the concentration of TNF-α found in sandwich ELISAs when compared with a standard curve. By measuring the amount of TNF-α in each sample, we were able to examine the relative amount of inflammation for each serum concentration and make connections to cellular stress and muscle atrophy.

3.5.2 QUANTIFICATION AND PURIFICATION OF RNA

Cell pellets were stored in Invitrogen TRIzol reagent (Thermo Fisher Scientific) for extraction of RNA at -20°C. In a small tube, 0.25 mL prepared mixture was added with 0.75 mL of TRIzol. The mixture was gently mixed and incubated at room temperature for 5 minutes to allow for complete dissociation of the nucleoproteins complex. After incubation, 115µL of chloroform was added to the tube and was thoroughly mixed and incubated for 3 minutes. The samples were then centrifuged for 15 minutes at 12,000 x g at 4º C. The mixture separated into a lower red phenol-chloroform, an interphase, and a colorless upper aqueous phase. The aqueous phase solution was transferred to new RNase free tubes via a pipettor. RNA was then isolated via precipitation, washing, and solubilization. Isolation began by adding 375µL of isopropanol to the tubes. This solution was incubated for 10 minutes at 4º C, then centrifuged for 10 minutes at 12,000 x g and 4º C. The supernatant that formed was discarded, and the pellet was resuspended in 750µL of 75% ethanol. The sample was briefly vortexed, and centrifuged for 5 minutes at 7,500 x g at 4º C. The supernatant was discarded, and the pellet was air dried for 10 minutes. The pellet was then resuspended in 50µL of RNase free water. RNA yields and purity were then

determined by use of a bio spectrometer. Absorbance at 260 nm determines total nucleic acid content, while absorbance at 280 nm provides sample purity. The RNA concentration was calculated by using the formula A260/A280 x dilution x 40 = µg RNA/mL.

3.5.3 QUALITATIVE PCR ANALYSIS AND GENE EXPRESSION

Six TaqMan Gene Expression Assays (96-well fast 0.1mL TaqMan array plates) (Thermo Fisher Scientific), were utilized to detect gene expression of several muscle atrophy biomarkers. These plates provided a qualitative assessment of gene regulation in each experimental context. While a 96-well plate was used, only 15 of the gene targets were utilized. The 6 samples used were 5% HS HSMM, 10% HS HSMM, 15% HS HSMM, 5% DHS D-HSMM, 10% DHS D-HSMM, and 15% DHS D-HSMM. TaqMan RNA-to-Ct 1-Step Kit (Thermo Fisher Scientific) was also used to convert RNA to Ct prior to using a standard cycle real time PCR (RT-PCR) system, Quant Studio 3 (Thermo Fisher Scientific). With a total volume of 20µL per reaction, 0.5µL of TaqMan RT-PCR enzyme mix (40x) was combined with 10µL of TaqMan RT-PCR Mix (2x) and 9.5µL of RNA template + RNase free water. The total volume of RNA was varied due to differing purified concentrations of each sample, seen in table 5. The cycling conditions were aligned to manufacturers protocol, outlined in table 6. Results were analyzed on Thermo Fisher Cloud. The 13 genes, along with two housekeeping genes were qualitatively analyzed from HSMM and D-HSMM cells plated in differing concentrations of human serum after 24 hours (Table 7). Relative abundance was measured based on the positive control reference plate, which were the HSMM cells plated with 10% HS. *Eukaryotic 18S rRNA* and *Actin alpha 1* were used as the housekeeping endogenous genes.

Sample	**RNA amount used per reaction**
HSMM 5% HS	87.5 ng/µL

HSMM 10% HS	115.9 ng/µL
HSMM 15% HS	99.5 ng/µL
D-HSMM 5% DHS	65.1 ng/µL
D-HSMM 10% DHS	58.7 ng/µL
D-HSMM 15% DHS	39.2 ng/µL

Table 5: RNA quantities used per each array plate

Step	Temperature	Duration	Cycles
Reverse transcription	48º C	15 minutes	Hold
Enzyme activation	95º C	10 minutes	Hold
Denaturation	95º C	15 seconds	40
Annealing/extension	60º C	1 minute	

Table 6: PCR cycling conditions

Gene name	Abbreviation
Eukaryotic 18S ribosomal RNA	18S
Actin alpha 1	ACTA1
Akt serine/threonine kinase 1	AKT1
Akt serine/threonine kinase 2	AKT2
Calpain 2	CAPN2
F-box protein 32 (Atrogin-1)	FBXO32
Forkhead box O1	FOXO1
Forkhead box O3	FOXO3
Insulin growth factor 1	IGF-1

Interleukin-1 beta	IL-1B
Interleukin-6	IL-6
Myostatin	MSTN
Protein kinase AMP-activated catalytic subunit alpha 1	PRKAA1
Ribosomal protein S6 kinase B1	RPS6KB1
Tumor Necrosis Factor	TNF-α

Table 7: Genes analyzed on TaqMan array plate

3.6 STATISTICAL ANALYSIS

Data values were taken in duplicate, biological samples were taken in triplicate. There were 3 biological replicates for each serum concentration and time for a total of 96 biological samples. All data was obtained from either 12-hour or 24-hour experiments. Each experiment contained a negative control (0% serum) and a positive control (10% serum). Data from PCR gene expression was qualitative, while the ELISA data was presented as mean ± standard error of the mean. The results among the different concentration, environment, time, and cell type were evaluated by preforming a 2-way analysis of variance (ANOVA) ($p<0.05$) and Tukey's post-hoc testing.

4. RESULTS

4.1 SKELETAL MUSCLE CELL VIABILITY

Cell viability for each treatment group are depicted in figures 3-6. Each figure represents the percentage of viable cells compared with the 10% FBS control. The values were normalized by dividing each treatment groups average means by the average mean of the 10% concentration in FBS for both 12 and 24 hours. Figure 3 compares the viability of HSMM cells plated with FBS. In this model, the data suggest that time ($p=0.0228$) and treatment serum concentration

(p=0.0045) have a significant effect on the variation in cell viability (table 8). Figure 4 compares the viability of D-HSMM cells plated with FBS. This model suggests that time has a-significant effect on the variation in cell viability (p=0.0026) (Table 9). Figure 5 compares the viability of HSMM cells plated with HS. This model suggests that treatment concentration (p<0.0001), time (p<0.0001), and the interaction of the two factors (p=0.0196) have a significant effect on variation in cell viability (table 10). Figure 6 compares the viability of D-HSMM cells plated with DHS. This model suggests that time accounts for a significant amount of variance in cell viability (p<0.001) but treatment concentration does not affect the model significantly (p=0.08) (table 11).

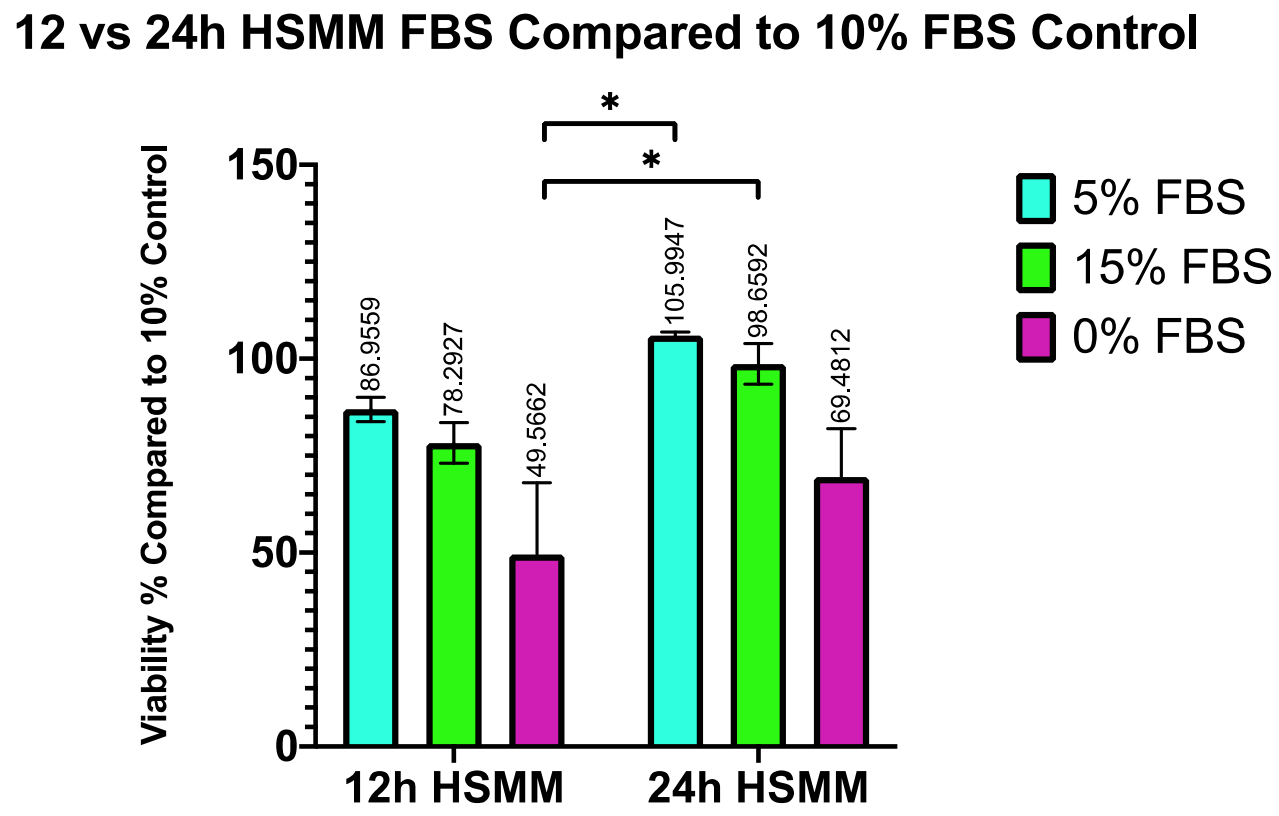

*Figure 3: 12 vs 24h HSMM cells in FBS compared with the 10% control. *= p-value<0.05, **=p-value<0.01 ***=p-value <0.001. Asterisks indicate individual comparisons.*

Source of Variation	% of total variation	P value	P value summary
Interaction	0.01455	0.9974	ns

Time	18.73	0.0228	*
Treatment concentration	48.28	0.0045	**

*Table 8: ANOVA Results of 12 vs 24h HSMM cells in FBS compared with the 10% control. This table represents the overall effects of this model. Alpha=0.05. *= p-value<0.05, **=p-value<0.01 ***=p-value <0.001*

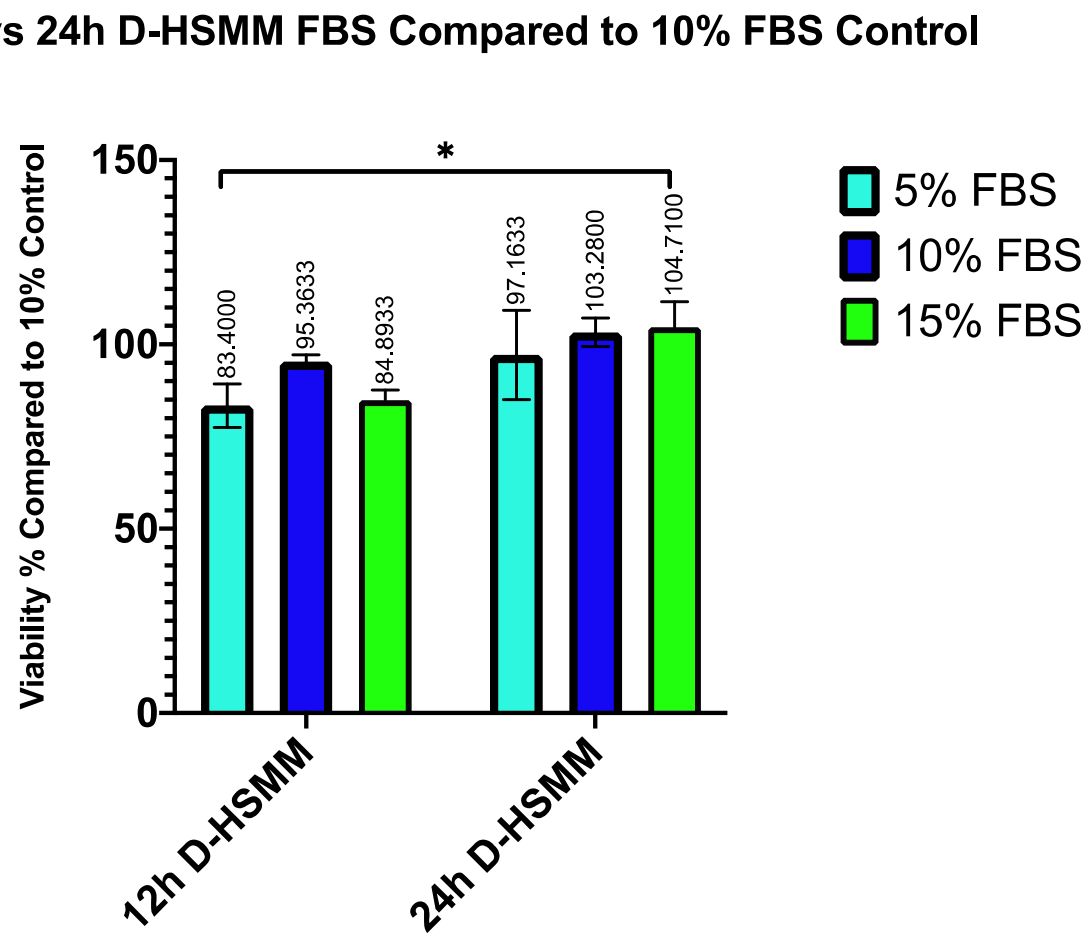

*Figure 4: 12 vs 24h D-HSMM cells in FBS compared with the 10% control. Alpha=0.05. *= p-value<0.05, **=p-value<0.01 ***=p-value <0.001. Asterisks indicate individual comparisons*

Source of Variation	% of total variation	P value	P value summary
Interaction	5.488	0.4394	ns
Time	44.48	0.0026	**
Treatment Concentration	12.67	0.1735	ns

*Table 9: ANOVA results of 12 vs 24h D-HSMM cells in FBS compared with 10% control. Alpha=0.05. *= p-value<0.05, **=p-value<0.01 ***=p-value <0.001.*

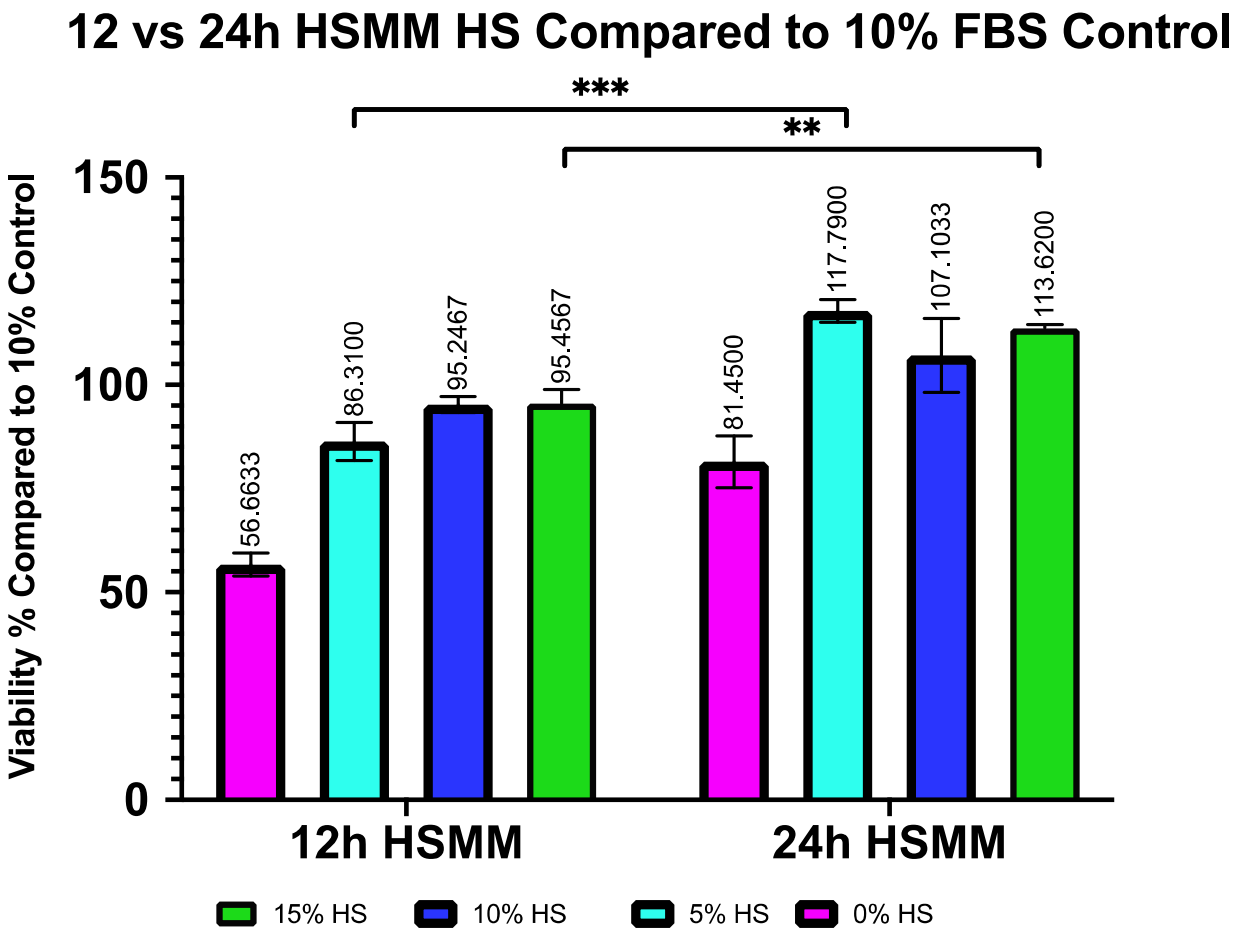

*Figure 5: 12 vs 24h HSMM cells in HS compared to 10% control. Alpha=0.05. *= p-value<0.05, **=p-value<0.01 ***=p-value <0.001. Asterisks indicate individual comparisons.*

Source of Variation	% of total variation	P value	P value summary
Interaction	3.741	0.0196	*
Time	32.46	<0.0001	****
Treatment concentration	59.25	<0.0001	****

*Table 10: ANOVA results of 12 vs 24h HSMM cells in HS compared to 10% control. Alpha=0.05. *= p-value<0.05, **=p-value<0.01 ***=p-value <0.001, ****=p-value<0.0001.*

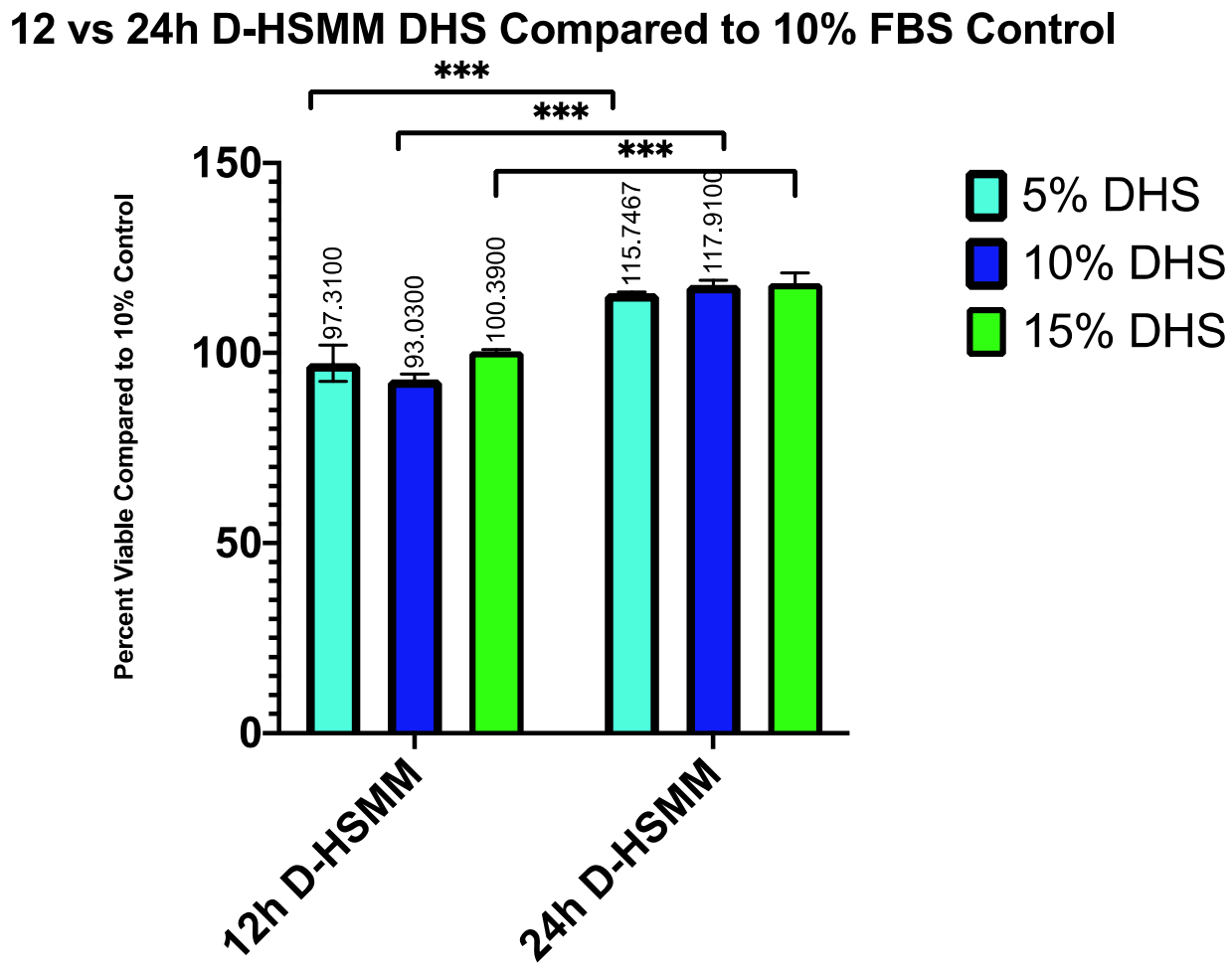

*Figure 6: 12 vs 24h D-HSMM cells in HS compared to 10% control. Alpha=0.05. *= p-value<0.05, **=p-value<0.01 ***=p-value <0.001. Asterisks indicate individual comparisons.*

Source of Variation	% of total variation	P value	P value summary
Interaction	2.179	0.1028	ns
Time	90.75	<0.0001	****
Treatment concentration	2.342	0.0894	ns

*Table 11: ANOVA results of 12 vs 24h D-HSMM cells in HS compared to 10% control. Alpha=0.05. *= p-value<0.05, **=p-value<0.01 ***=p-value <0.001, ****=p-value<0.0001.*

4.2 OXIDATIVE STRESS

Superoxide dismutase 1 concentrations for each treatment group are shown in tables 12-15. The tables represent the concentration in pg/mL. These levels were then normalized against the HSMM 10% for each media type. Figures 7-9 represent the percentage of each treatment group from the control, which is represented as 100%. As serum concentration increases, the level of SOD1 present in the human serum samples for both HSMM and D-HSMM also increases (table 12 and 13).

	5% HS	10% HS	15% HS
HSMM 12 h	8149.42 ±503.83 [a]	13497.27± 244.01 [b]	17731.26± 1238.12 [b]
HSMM 24 h	8074.86± 655.21 [c]	15910.25± 628.10 [d]	19170.465735± 6.78 [d]

Table 12: Mean ± SEM SOD1 concentration in 12 vs. 24-hour HSMM cells in HS. Numbers are represented as mean concentration ± SEM of SOD1 in pg/mL. Data in rows that share different letter superscripts are significantly different ($p<0.05$)

	5% DHS	10% DHS	15% DHS
D-HSMM 12h	12729.09 ± 271.12[a]	18625 ± 54.22 [b]	21090.9 ± 851.76 [b]
D-HSMM 24h	11289.9 ± 621.31 [c]	18867.71 ± 192.04 [d]	20761.03 ± 630.35 [d]

Table 13: Mean ± SEM SOD1 Concentration in 12 vs 24-hour D-HSMM cells plated in human serum. Numbers are represented as mean concentration ± SEM of SOD1 in pg/mL. Data in rows that share different letter superscripts are significantly different ($p<0.05$)

In HSMM cells plated with FBS, treatment concentration showed a significant effect on SOD1 concentration (p=0.0084), seen in table 14. Table 15 depicts the mean SOD1 concentration in D-HSMM cells plated with FBS, no significance was noted.

	5% FBS	10% FBS	15% FBS
HSMM 12h	135.63 ± 13.01 [a]	81.748 ± 22.29 [a]	200.65 ±22.29 [b]
HSMM 24h	215.52 ± 14.86 [c]	126.34 ±11.147 [c]	131.91 ± 5.57 [c]

Table 14: Mean ± SEM SOD1 Concentration in 12 vs 24-hour HSMM cells plated in FBS. Numbers are represented as mean concentration ± SEM of SOD1 in pg/mL. Data in rows that share different letter superscripts are significantly different (p<0.05)

	5% FBS	10% FBS	15% FBS
D-HSMM 12 h	193.22 ± 22.30 [a]	386.12 ± 152.35 [a]	486.78 ±326.99 [a]
D-HSMM 24 h	204.37 ± 40.87 [b]	204.37 ± 52.02 [b]	204.37 ± 81.75 [b]

Table 15: Mean SOD1 concentration in 12 vs 24h D-HSMM cells in FBS. Numbers are represented as mean concentration ± SEM of SOD1 in pg/mL. Data in rows that share different letter superscripts are significantly different (p<0.05)

When the data is normalized against a control, both HSMM and D-HSMM FBS models were not significantly affected by time nor treatment concentration (tables 16 and 17). In the HSMM FBS model, however, serum concentration accounted for 39.84% of variation in the model, although insignificant (p=0.0787) (table 16). The data suggests there was a SOD1 decrease from 12 to 24 hours in the D-HSMM FBS model. The ANOVA results from normalized HSMM and D-HSMM HS/DHS SOD1 suggest that both time and treatment concentration accounted for a significant effect in variation in these models. The significant stepwise increase in SOD1 levels in both HS and DHS experiments (tables 18 and 19) may be confounded by exogenous SOD1 already present in the HS.

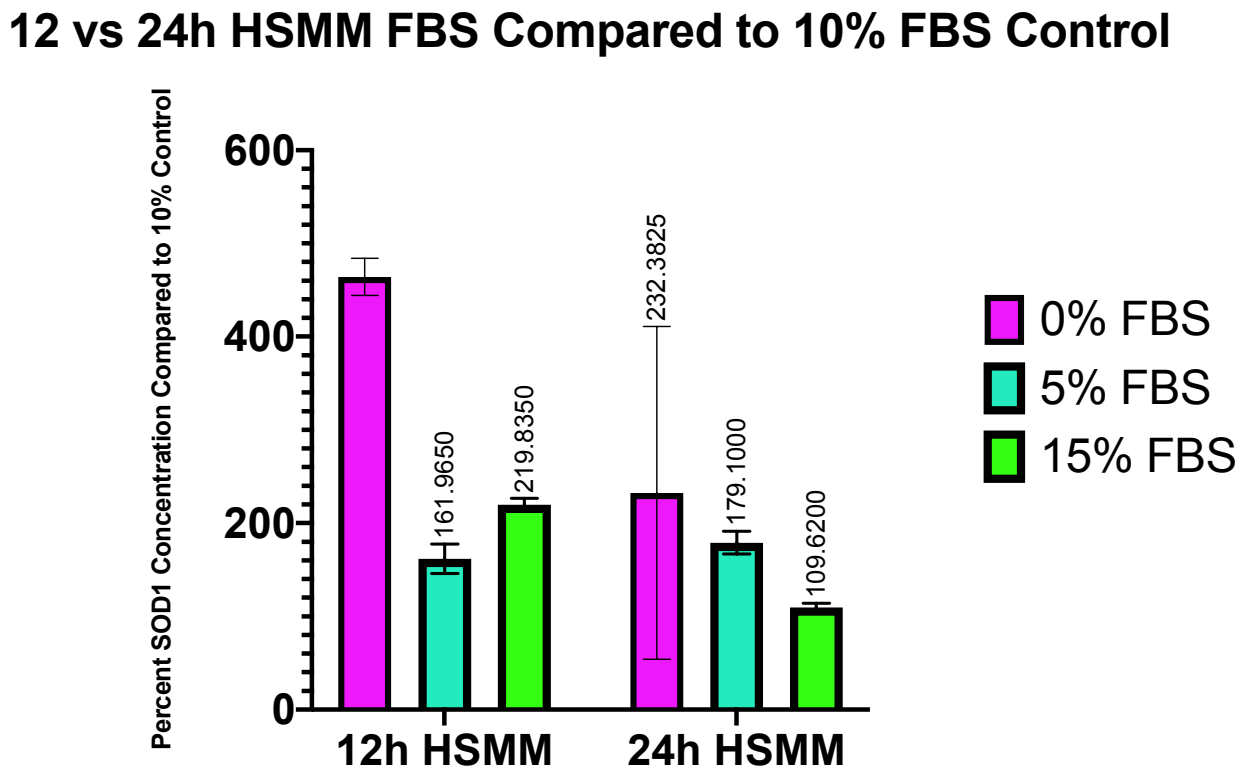

Figure 7: 12 vs 24h HSMM FBS Compared to 10% FBS control

Source of Variation	% of total variation	P value	P value summary
Interaction	14.18	0.312	ns
Time	16.1	0.1223	ns
Treatment Concentration	39.84	0.0787	ns

Table 16: ANOVA results of 12 vs 24h HSMM FBS Compared to 10% FBS control

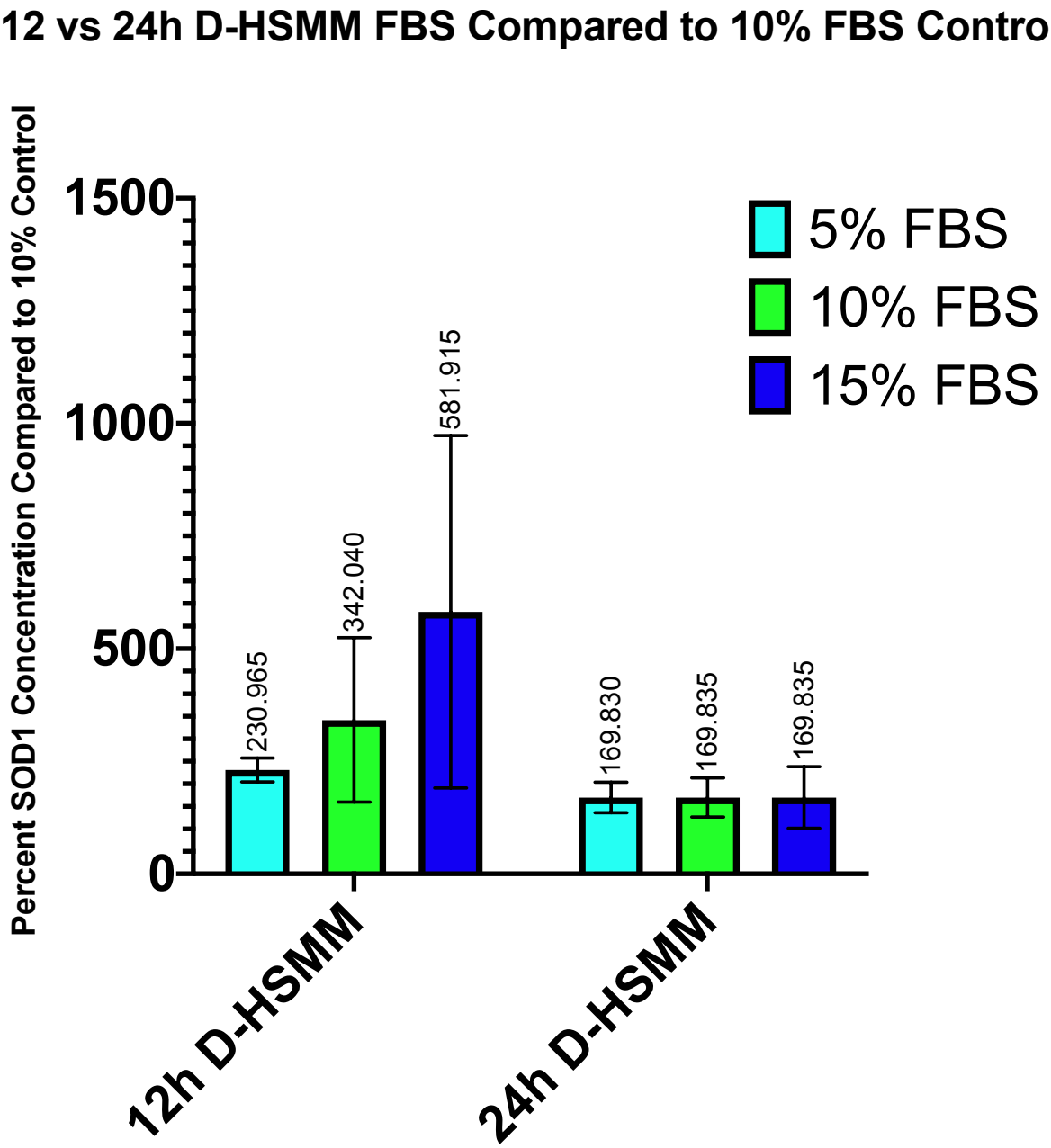

*Figure 8: 12 vs 24h D-HSMM FBS Compared to 10% FBS control. Alpha=0.05. *= p-value<0.05, **=p-value<0.01 ***=p-value <0.001. Asterisks indicate individual comparisons.*

Source of Variation	% of total variation	P value	P value summary
Interaction	9.806	0.6315	ns
Time	21.16	0.1935	ns
Treatment Concentration	9.806	0.6315	ns

*Table 17: ANOVA results of 12 vs 24h D-HSMM FBS compared to 10% FBS control. Alpha=0.05. *= p-value<0.05, **=p-value<0.01 ***=p-value <0.001.*

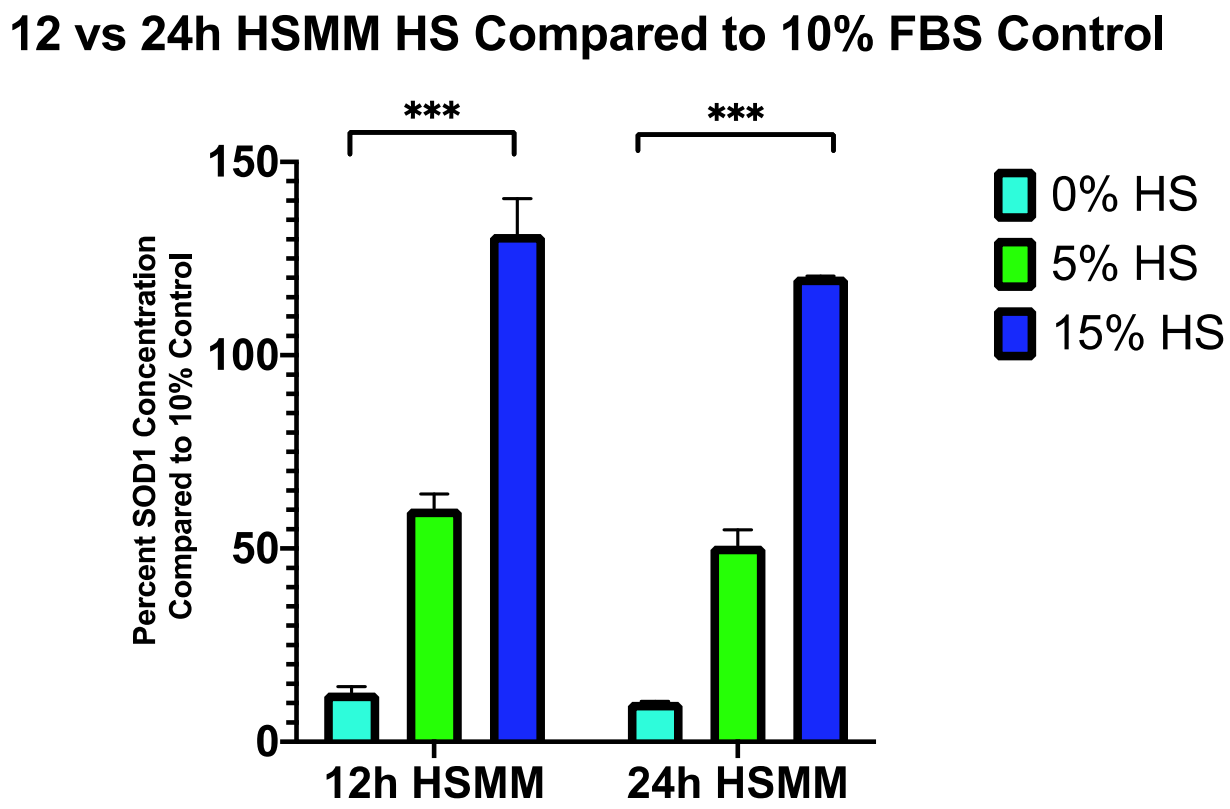

*Figure 9: 12 vs 24h HSMM HS compared to 10% HS control. Alpha=0.05. *= p-value<0.05, **=p-value<0.01 ***=p-value <0.001. Asterisks indicate individual comparisons.*

Source of Variation	% of total variation	P value	P value summary
Interaction	0.1573	0.607	ns
Time	0.6506	0.0783	ns
Treatment concentration	98.32	<0.0001	****

*Table 18: ANOVA results of 12 vs 24h HSMM HS compared to 10% HS control. Alpha=0.05. *= p-value<0.05, **=p-value<0.01 ***=p-value <0.001, ****=p-value<0.0001.*

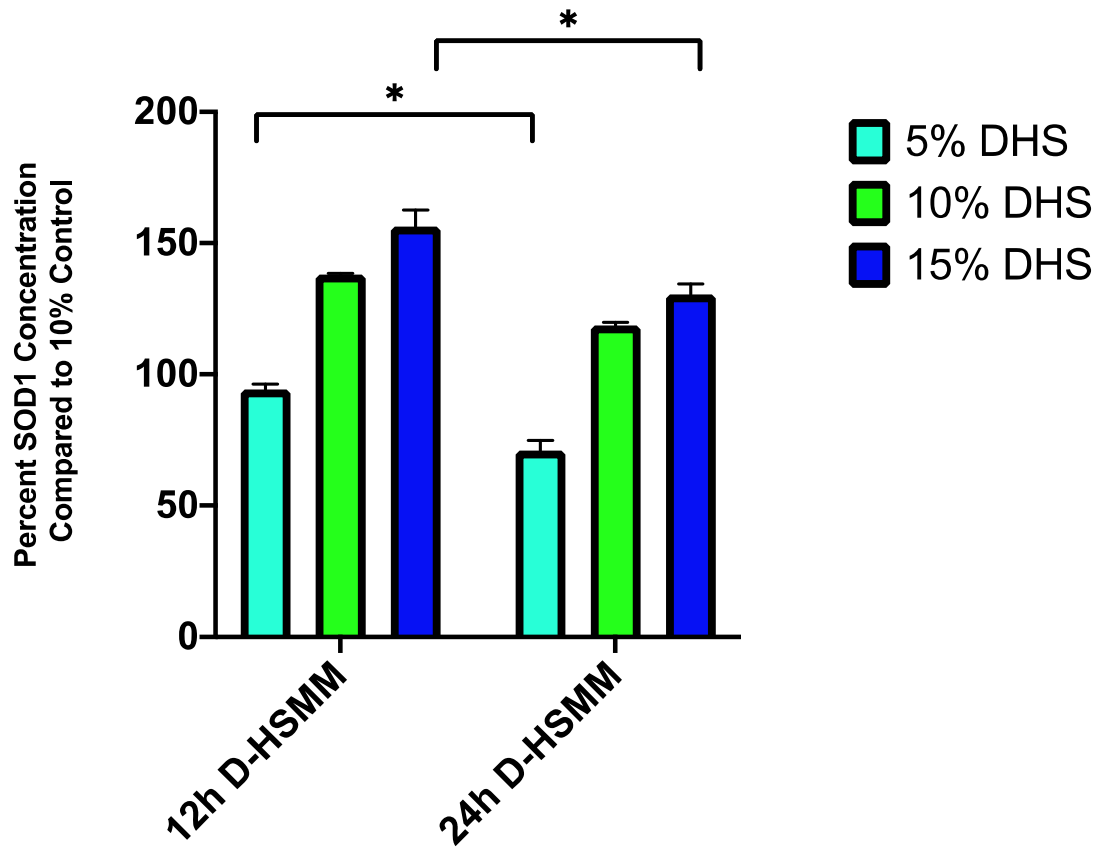

*Figure 10: 12 vs 24h D-HSMM DHS compared to 10% HS control. Alpha=0.05. *= p-value<0.05, **=p-value<0.01 ***=p-value <0.001. Asterisks indicate individual comparisons.*

Source of Variation	% of total variation	P value	P value summary
Interaction	0.2118	0.6843	ns
Time	16.07	0.0002	***
Treatment concentration	82.15	<0.0001	****

*Table 19: ANOVA results of12 vs 24h D-HSMM DHS compared to 10% HS control. Alpha=0.05. *= p-value<0.05, **=p-value<0.01 ***=p-value <0.001, ****=p-value<0.0001.*

4.3 ATROGIN-1 PRESENCE IN SERUM

There was no significant evidence that Atrogin-1 (FBXO32) was present in serum. This was reflected by virtually no signal of Atrogin-1 in every treatment and control group compared to the standard curve.

4.4 TUMOR NECROSIS FACTOR ALPHA PRESENCE IN SERUM

Tumor Necrosis Factor Alpha levels in serum did not reveal any patterns consistent with current literature. Tables 20-23 reflect the mean value ± SEM of TNF-α concentration in pg/mL. A 2-way ANOVA of this data suggests that in HSMM models plated with FBS, TNF-α concentration significantly decreased from 12 to 24 hours ($p=0.0261$). This analysis also suggests that there was no significant observed effect of treatment concentration on this model. However, there was an observed slight decrease in TNF-α concentration from 12 to 24 hours, although this interaction was insignificant ($p=0.84$). In D-HSMM models plated with FBS, there was no observed significant effect from treatment concentration or time. The interaction between these two factors was also not significant. There was a slight increase in TNF-α concentration seen in 5% FBS, although this was also not significant ($p= 0.7$).

	5% FBS	**10% FBS**	**15% FBS**
HSMM 12 h	18.76 ± 1.94^{a}	9.0575 ± 3.8825^{a}	9.0555 ± 5.1745^{a}
HSMM 24 h	3.24 ± 3.24^{b}	5.805 ± 5.805^{b}	0 ± 0.0

Table 20: Mean ± SEM TNF-α concentration in 12 vs. 24-hour HSMM cells plated with FBS. Numbers are represented as mean concentration ± SEM of SOD1 in pg/mL. Data in rows that share the same letter superscripts are not significantly different ($p<0.05$)

	5% FBS	**10% FBS**	**15% FBS**
D-HSMM 12 h	3.234 ± 0.0647^{a}	4.528 ± 4.528^{a}	7.74 ± 2.565^{a}
D-HSMM 24 h	7.762 ± 0.0^{b}	3.234 ± 0.647^{b}	3.23 ± 3.23^{b}

Table 21: Mean ± SEM TNF-α concentration in 12 vs. 24-hour D-HSMM cells plated with FBS. Numbers are represented as mean concentration ± SEM of SOD1 in pg/mL. Data in rows that share the same letter superscripts are not significantly different ($p<0.05$). Data with zeroes indicate no signal from assay.

	5% HS	10% HS	15% HS
HSMM 12 h	2.4799±0.8266[a]	6.6130±0.0[a]	6.6130±1.6532[a]
HSMM 24 h	0±0.0	0±0.0	11.5728±4.9597

Table 22: Mean ± SEM TNF-α levels in 12 vs. 24-hour HSMM cells plated with HS. Numbers are represented as mean concentration ± SEM of SOD1 in pg/mL. Data in rows that share same letter superscripts are not significantly different ($p<0.05$). Data with zeroes indicate no signal from assay.

	5% DHS	10% DHS	15% DHS
D-HSMM 12 h	4.9598±4.9598	0±0.0	0±0.0
D-HSMM 24 h	0±0.0	0±0.0	0±0.0

Table 23: Mean ± SEM TNF-α levels in 12 vs. 24-hour D-HSMM cells plated with DHS. Numbers are represented as mean concentration ± SEM of SOD1 in pg/mL. Data with zeroes indicate no signal from assay.

When the data was normalized against the 10% HSMM FBS control, both HSMM and D-HSMM FBS models (seen in figures 11 and 12) were not significantly affected by time nor treatment concentration (tables 24 and 25). However, the percentage of TNF-α in the 5% HSMM FBS treatment group was higher or equal to the amount found in 10% HSMM FBS. In human serum models (figures 13 and 14) no significant effects were observed for the time variable. The HSMM HS model depicts a significant effect of treatment concentration ($p=0.0116$) (table 26). In both HSMM and D-HSMM human serum models, there was very low signal of TNF-α present in serum compared to the standard curve, with some concentrations not producing any detectable amount (figure 14).

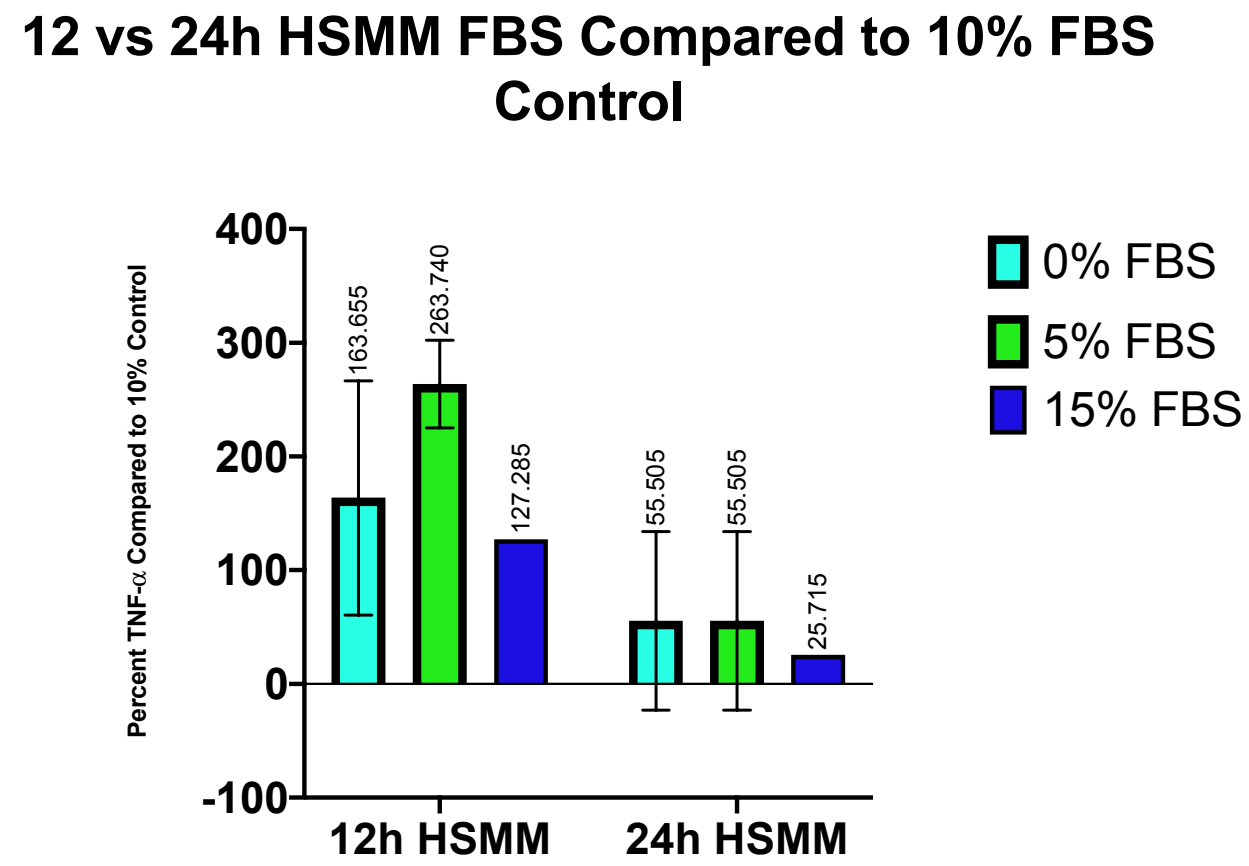

*Figure 11: 12 vs 24h HSMM FBS Compared to 10% FBS Control. Alpha=0.05. *= p-value<0.05, **=p-value<0.01 ***=p-value <0.001. Asterisks indicate individual comparisons.*

Source of Variation	% of total variation	P value	P value summary
Interaction	6.177	0.5833	ns
Time	50.33	0.0211	*
Treatment Concentration	12.11	0.3757	ns

*Table 24: ANOVA results of 12 vs 24h HSMM FBS Compared to 10% FBS Control. Alpha=0.05. *= p-value<0.05, **=p-value<0.01 ***=p-value <0.001.*

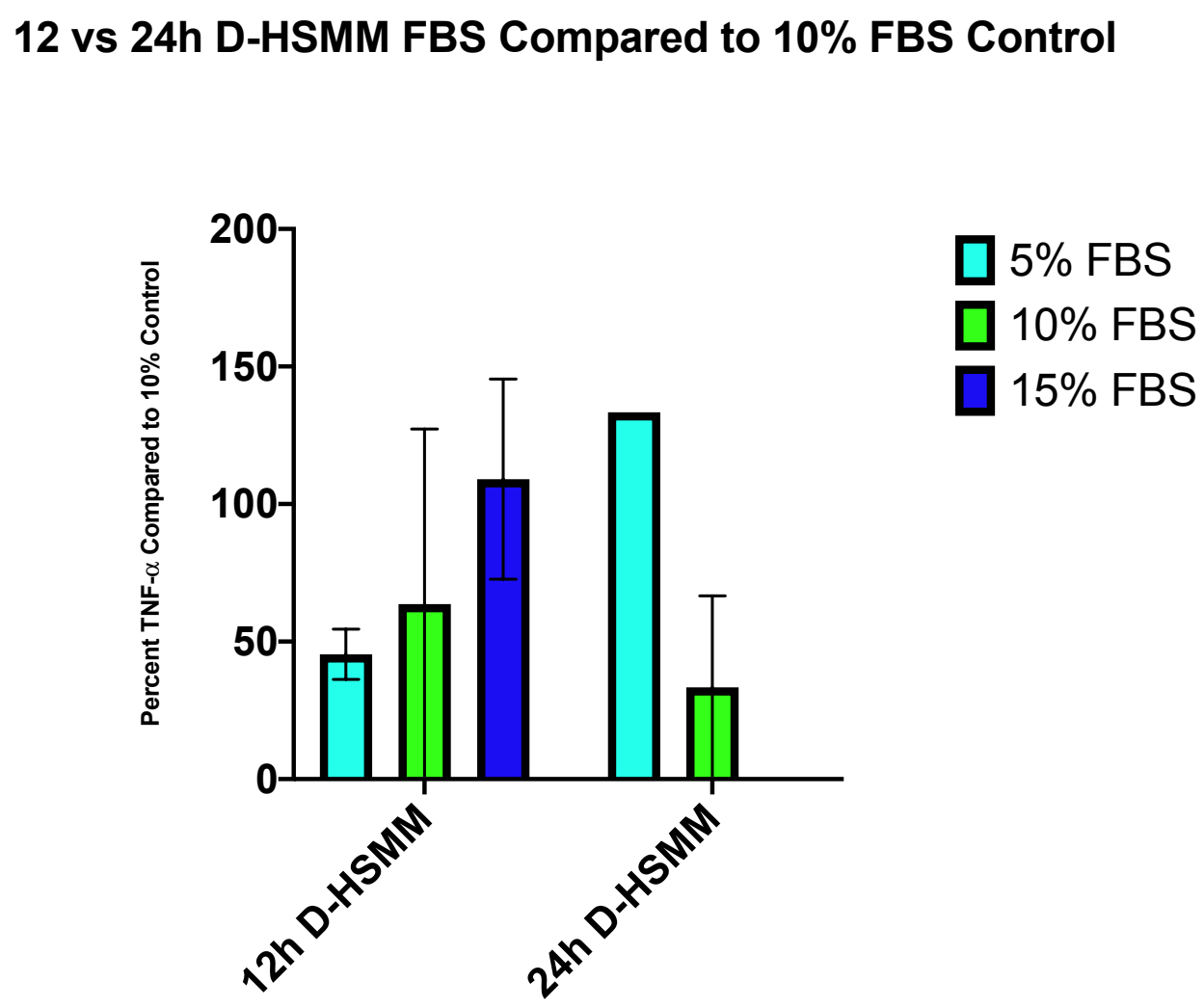

*Figure 12: 12 vs 24h D-HSMM FBS Compared to 10% FBS control. Alpha=0.05. *= p-value<0.05, **=p-value<0.01 ***=p-value <0.001. No bar present in the 24h 15% indicates no signal from assay.*

Source of Variation	% of total variation	P value	P value summary
Interaction	52.31	0.0643	ns
Time	2.347	0.5491	ns
Treatment Concentration	10.38	0.4585	ns

*Table 25: ANOVA results of 12 vs 24h D-HSMM FBS Compared to 10% FBS Control. Alpha=0.05. *= p-value<0.05, **=p-value<0.01 ***=p-value <0.001.*

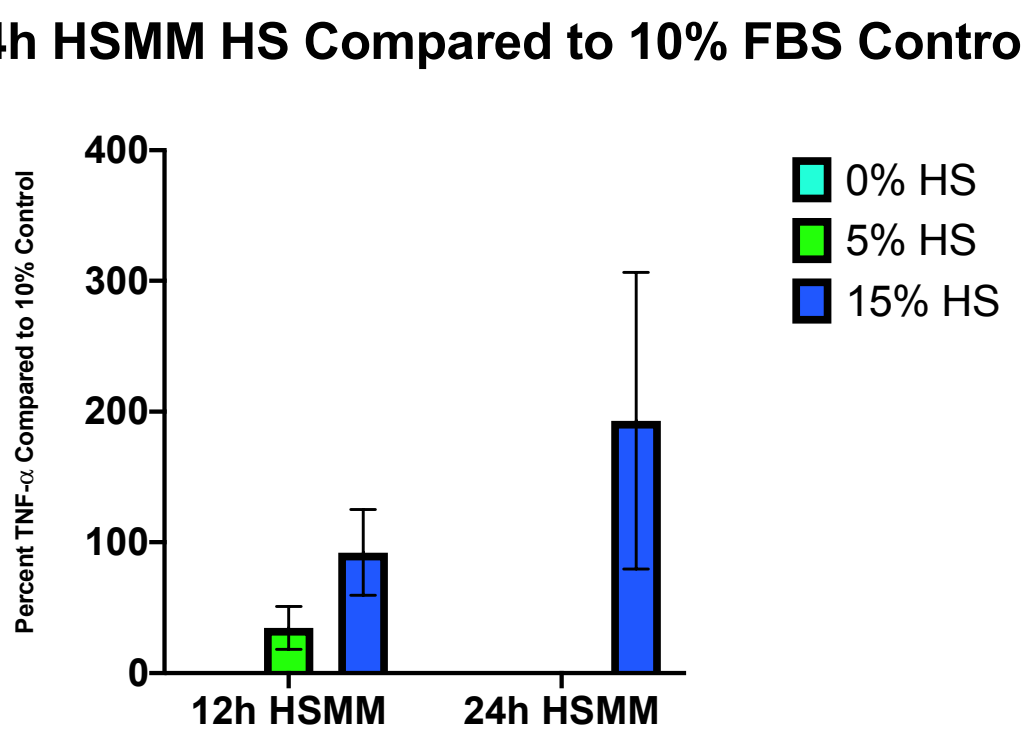

*Figure 13: 12 vs 24h HSMM HS compared to 10% FBS control. Alpha=0.05. *= p-value<0.05, **=p-value<0.01 ***=p-value <0.001. No bar present in the 12h 0%, 24h 0%, 24h 5% and 24h 15% indicates no signal from assay.*

Source of Variation	% of total variation	P value	P value summary
Interaction	13.36	0.2047	ns
Time	1.971	0.462	ns
Treatment Concentration	65.51	0.0116	*

*Table 26: ANOVA results of 12 vs 24h HSMM HS compared to 10% FBS control. Alpha=0.05. *= p-value<0.05, **=p-value<0.01 ***=p-value <0.001.*

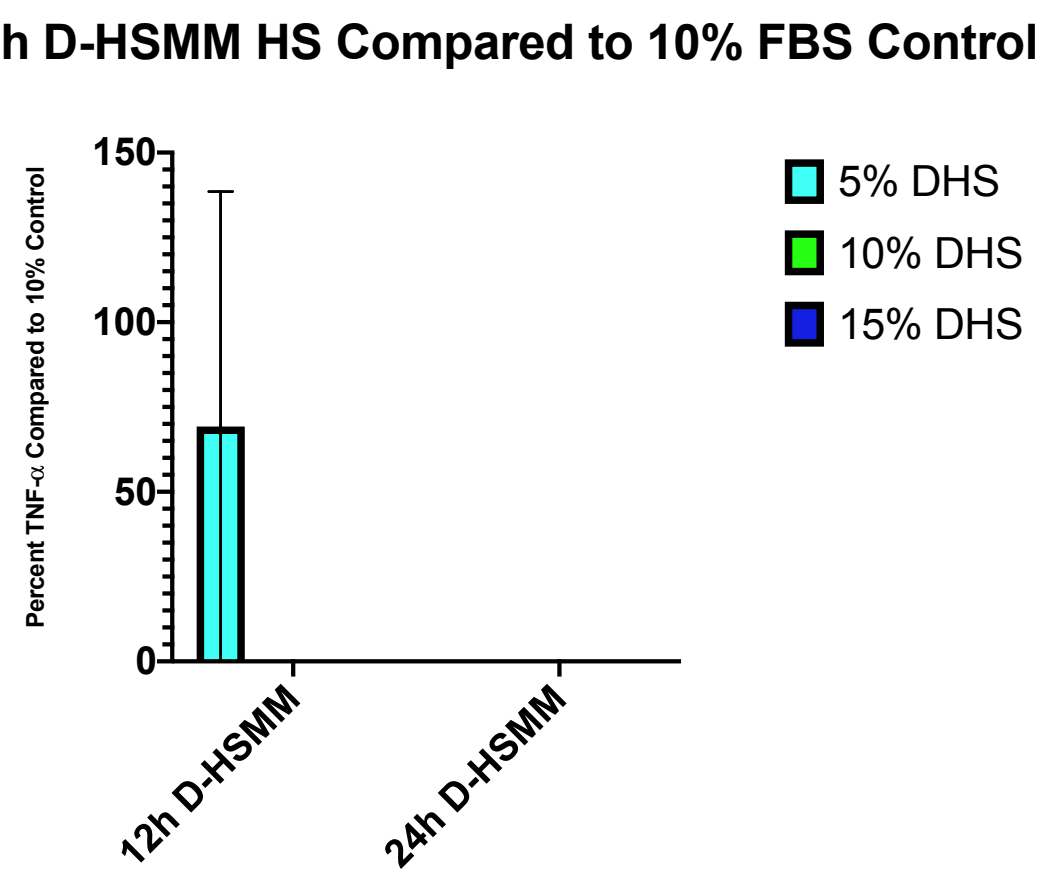

*Figure 14: 12 vs 24h D-HSMM HS compared to 10% FBS control. Alpha=0.05. *= p-value<0.05, **=p-value<0.01 ***=p-value <0.001. No bar present in the 12h 10%, 12h 15%, 24h 5%, 24h 10% and 24h 15% indicates no signal from assay.*

Source of Variation	% of total variation	P value	P value summary
Interaction	18.18	0.4219	ns
Time	9.091	0.3559	ns
Treatment Concentration	18.18	0.4219	ns

*Table 27: ANOVA results of 12 vs 24h D-HSMM HS compared to 10% FBS control. Alpha=0.05. *= p-value<0.05, **=p-value<0.01 ***=p-value <0.001.*

4.5 DATA NORMALIZED AGAINST DIABETIC CONTROL

4.5.1 CELL VIABILITY

The data reported above was also normalized against the 10% FBS D-HSMM, as a control. Percent viability is represented in figures 15-18 and tables 28-31. Individual effects were noted by asterisk on figures. Treatment concentration was a significant source of variation in HSMM FBS model (p=0.0007) (table. 28). Time and treatment concentration also significantly affected the HSMM HS model, with both p-values < 0.0001 (table 30). The D-HSMM DHS model depicts time as a significant source of variation (p<0.0001) (table 31).

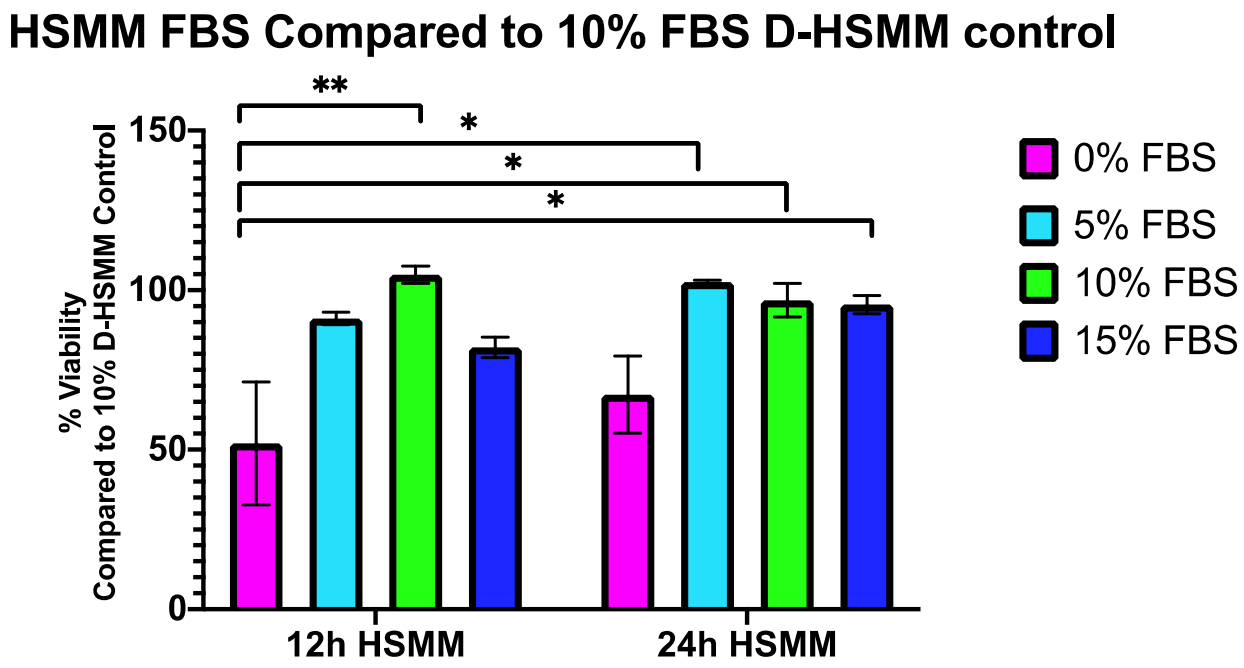

*Figure 15: Percent viability of 12 vs 24h HSMM FBS compared to D-HSMM 10% FBS control. Alpha=0.05. *= p-value<0.05, **=p-value<0.01 ***=p-value <0.001.*

Source of Variation	% of total variation	P value	P value summary
Interaction	4.927	0.5081	ns
Time	3.675	0.1977	ns
Treatment Concentration	58.85	0.0007	***

*Table 28: ANOVA results of 12 vs 24h HSMM FBS compared to D-HSMM 10% FBS control. Alpha=0.05. *= p-value<0.05, **=p-value<0.01 ***=p-value <0.001.*

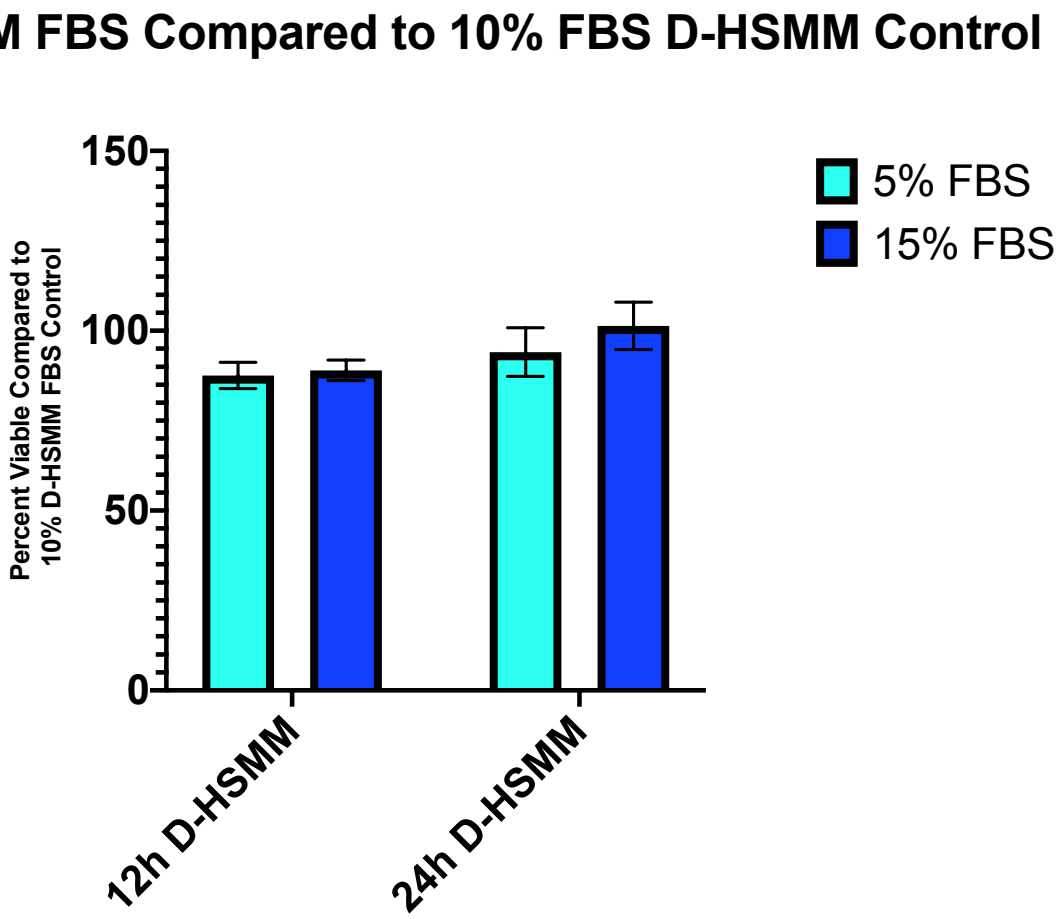

*Figure 16: Percent viability of 12 vs 24h D-HSMM FBS compared to D-HSMM 10% FBS control. Alpha=0.05. *= p-value<0.05, **=p-value<0.01 ***=p-value <0.001.*

Source of Variation	% of total variation	P value	P value summary
Interaction	2.522	0.5948	ns
Time	26.13	0.1125	ns
Treatment Concentration	5.583	0.4338	ns

*Table 29: ANOVA results of 12 vs 24h D-HSMM FBS compared to D-HSMM 10% FBS control. Alpha=0.05. *= p-value<0.05, **=p-value<0.01 ***=p-value <0.001.*

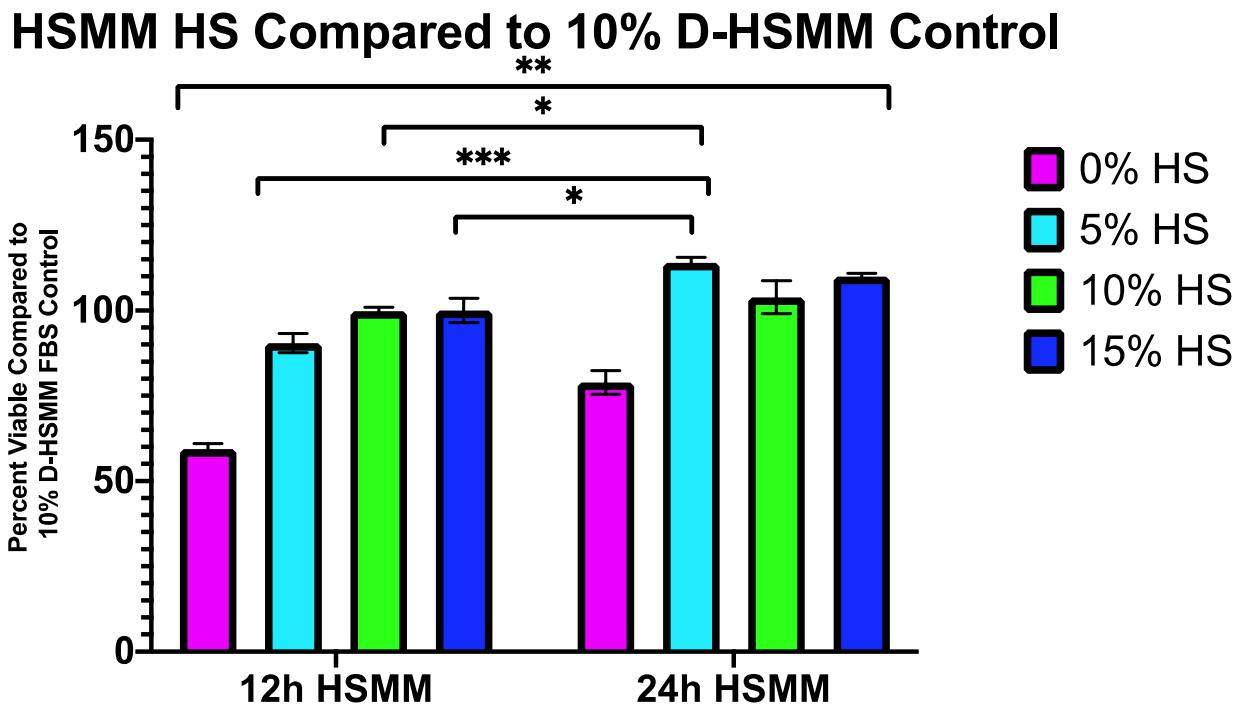

*Figure 17: Percent viability of 12 vs 24h HSMM HS compared to D-HSMM 10% FBS control. Alpha=0.05. *= p-value<0.05, **=p-value<0.01 ***=p-value <0.001.*

Source of Variation	% of total variation	P value	P value summary
Interaction	4.953	0.0126	*
Time	17.03	<0.0001	****
Treatment Concentration	72.7	<0.0001	****

*Table 30: ANOVA results of 12 vs 24h HSMM HS compared to D-HSMM 10% FBS control. Alpha=0.05. *= p-value<0.05, **=p-value<0.01 ***=p-value <0.001, ****=p-value<0.0001.*

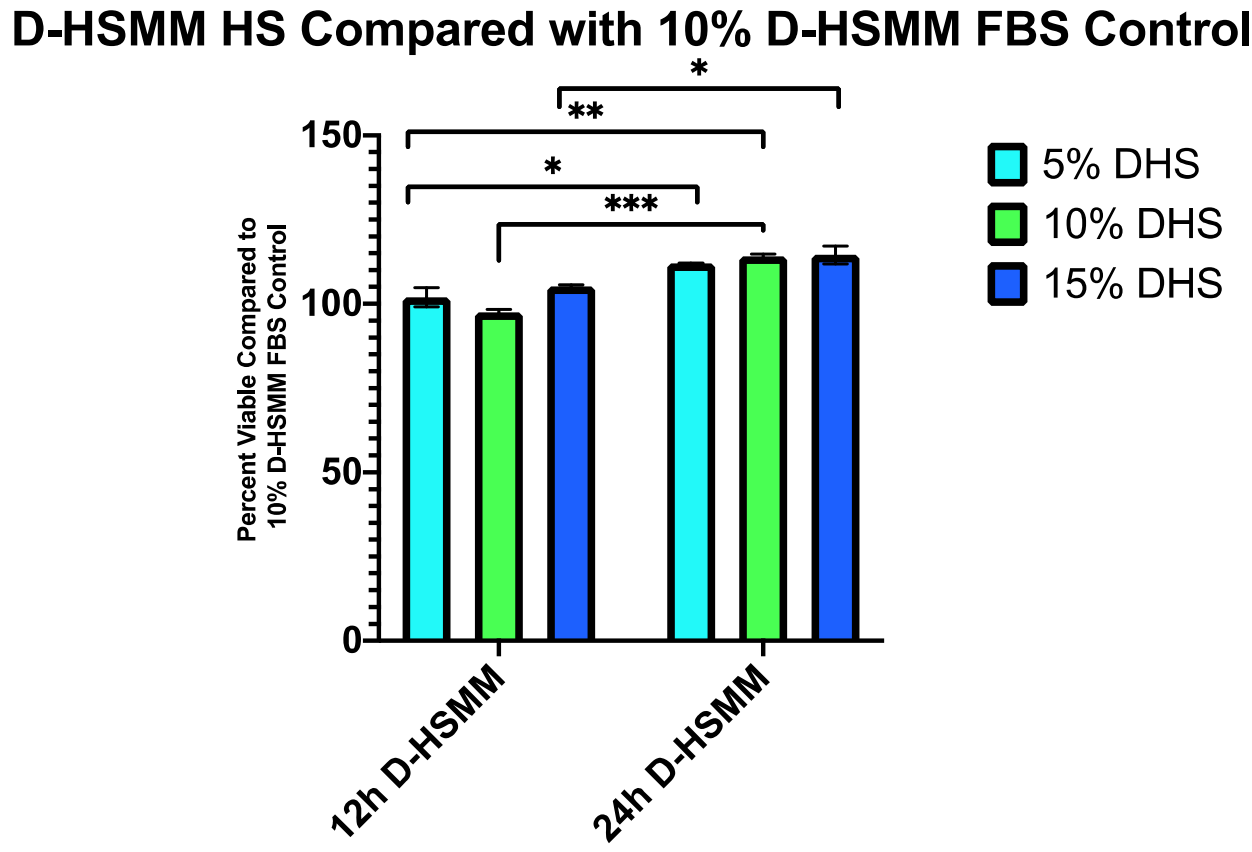

*Figure 18: Percent viability of 12 vs 24h D-HSMM HS compared to D-HSMM 10% FBS control. Alpha=0.05. *= p-value<0.05, **=p-value<0.01 ***=p-value <0.001.*

Source of Variation	% of total variation	P value	P value summary
Interaction	5.743	0.0915	ns
Time	76.38	<0.0001	****
Treatment Concentration	6.144	0.0799	ns

*Table 31: ANOVA results of 12 vs 24h D-HSMM DHS compared to D-HSMM 10% FBS control. Alpha=0.05. *= p-value<0.05, **=p-value<0.01 ***=p-value <0.001, ****=p-value<0.0001.*

4.5.2 SUPEROXIDE DISMUTASE 1

SOD1 values normalized against the diabetic control are shown below in tables 32-35 and figures 19-22. These values were normalized against the 10% FBS and 10% DHS, respectively. A significant effect of time (p=0.001) and treatment concentration (p<0.0001) was

noted in the HSMM FBS model (table 32). Treatment concentration accounted for a significant effect on variation in both HSMM and D-HSMM human serum models, with both p values <0.0001 (tables 34 and 35).

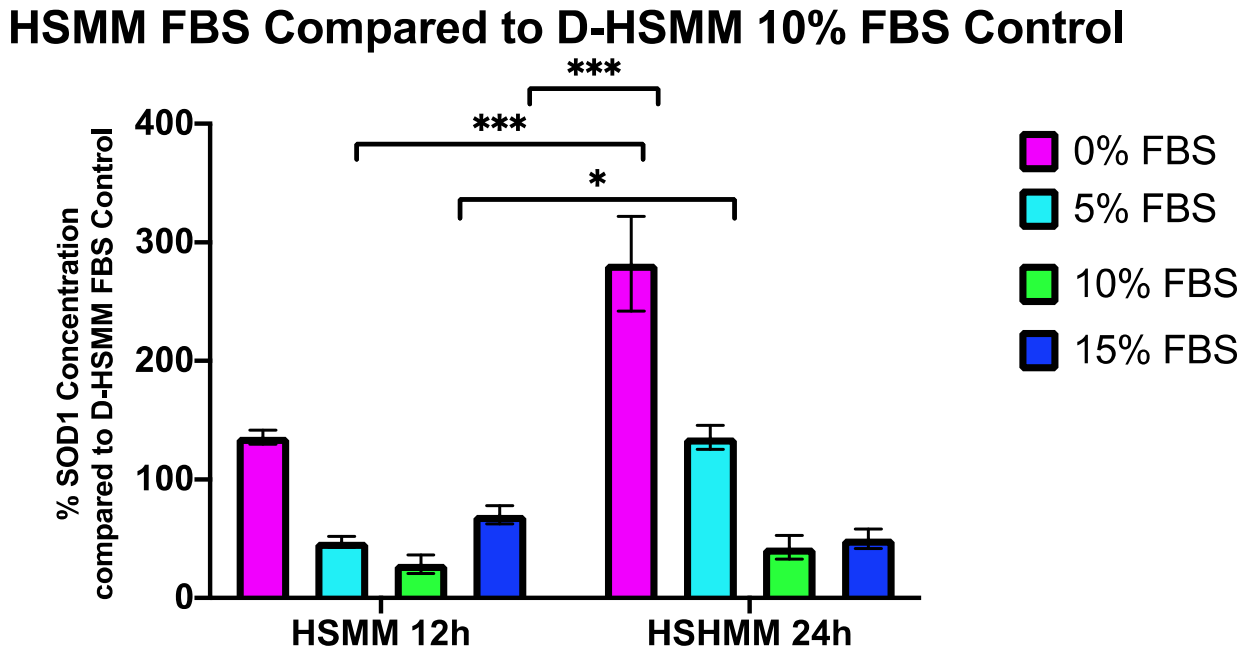

*Figure 19: Normalized SOD1 values of 12 vs 24h HSMM FBS compared to D-HSMM 10% FBS control. Alpha=0.05. *= p-value<0.05, **=p-value<0.01 ***=p-value <0.001.*

Source of Variation	% of total variation	P value	P value summary
Interaction	16	0.0034	**
Time	12.48	0.001	***
Treatment Concentration	67.61	<0.0001	****

*Table 32: ANOVA results of 12 vs 24h HSMM FBS compared to D-HSMM 10% FBS control. Alpha=0.05. *= p-value<0.05, **=p-value<0.01 ***=p-value <0.001, ****=p-value<0.0001.*

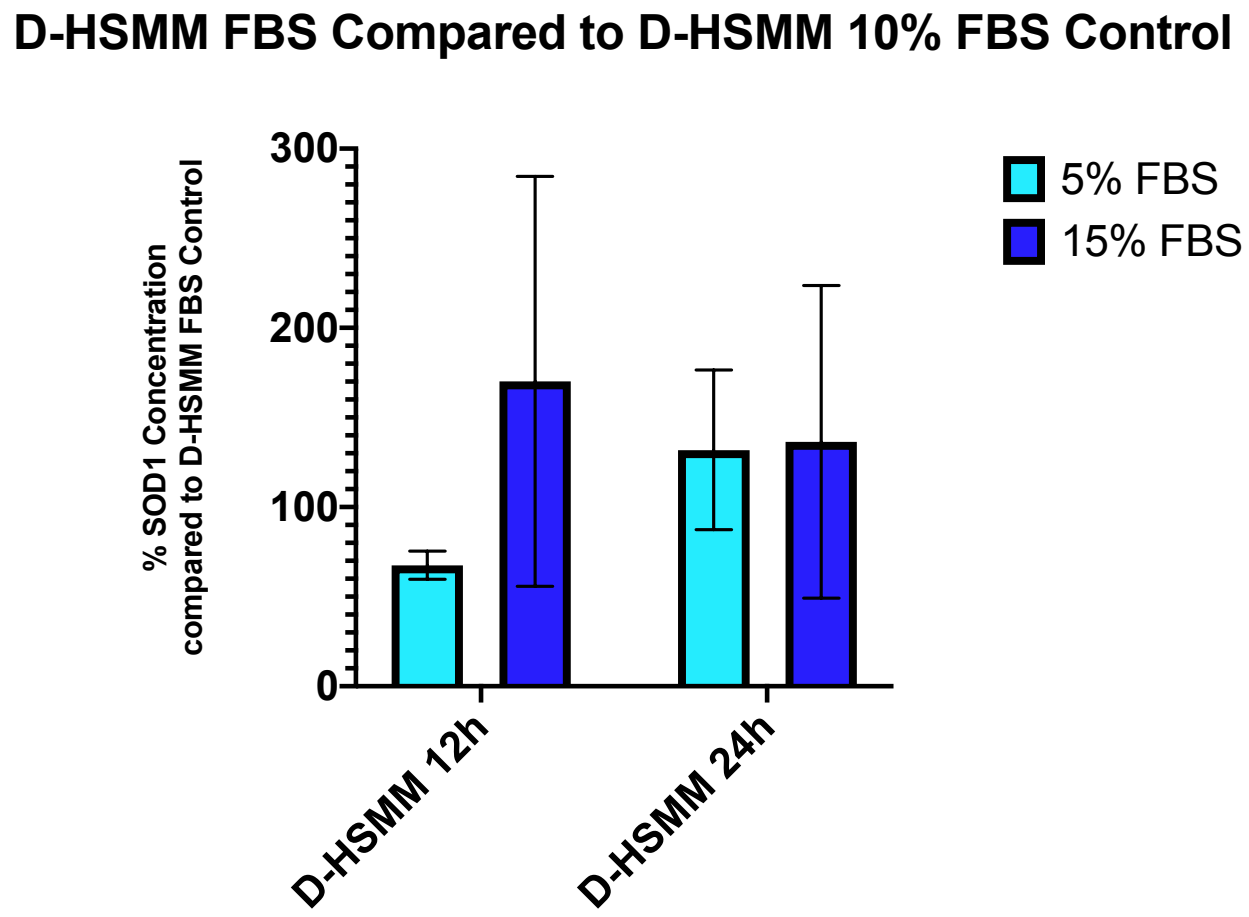

*Figure 20: Normalized SOD1 values of 12 vs 24h D-HSMM FBS compared to D-HSMM 10% FBS control. Alpha=0.05. *= p-value<0.05, **=p-value<0.01 ***=p-value <0.001.*

Source of Variation	% of total variation	P value	P value summary
Interaction	8.514	0.5509	ns
Time	0.8249	0.8494	ns
Treatment Concentration	10.17	0.5165	ns

*Table 33: ANOVA results of 12 vs 24h D-HSMM FBS compared to D-HSMM 10% FBS control. Alpha=0.05. *= p-value<0.05, **=p-value<0.01 ***=p-value <0.001.*

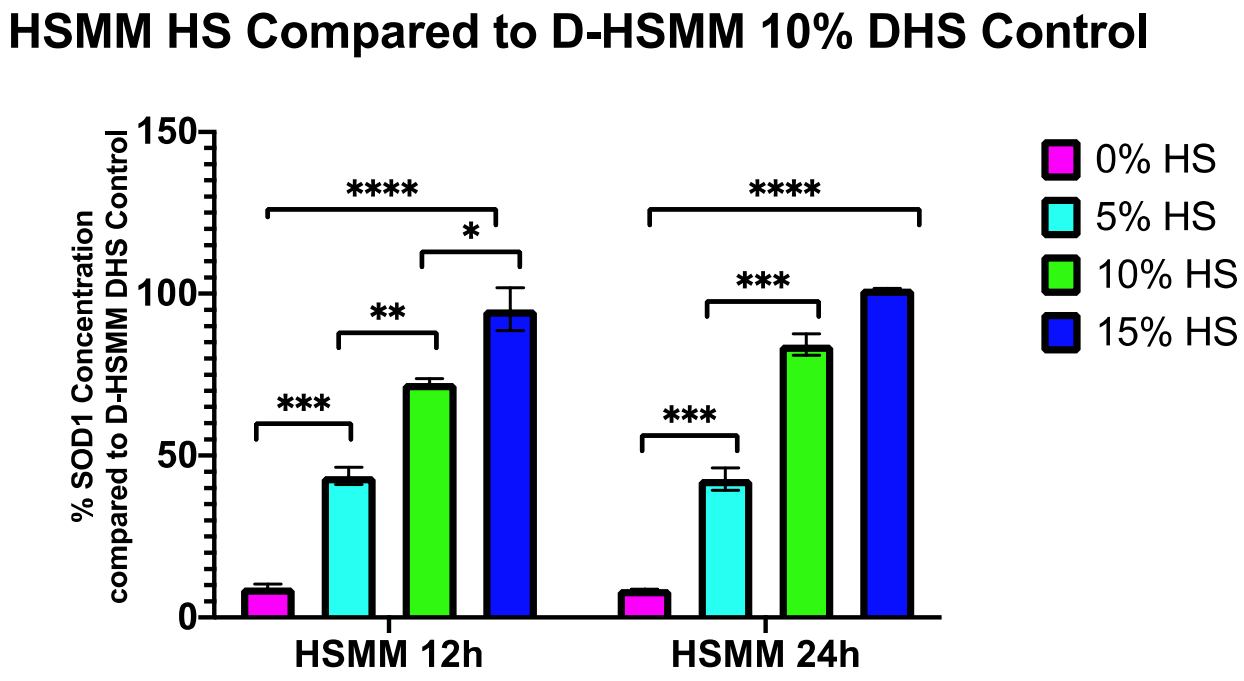

*Figure 21: Normalized SOD1 values of 12 vs 24h HSMM HS compared to D-HSMM 10% DHS control. Alpha=0.05. *= p-value<0.05, **=p-value<0.01 ***=p-value <0.001.*

Source of Variation	% of total variation	P value	P value summary
Interaction	0.5929	0.2028	ns
Time	0.3705	0.0934	ns
Treatment Concentration	98.22	<0.0001	****

*Table 34: ANOVA results of 12 vs 24h HSMM HS compared to D-HSMM 10% DHS control. Alpha=0.05. *= p-value<0.05, **=p-value<0.01 ***=p-value <0.001, ****=p-value<0.0001.*

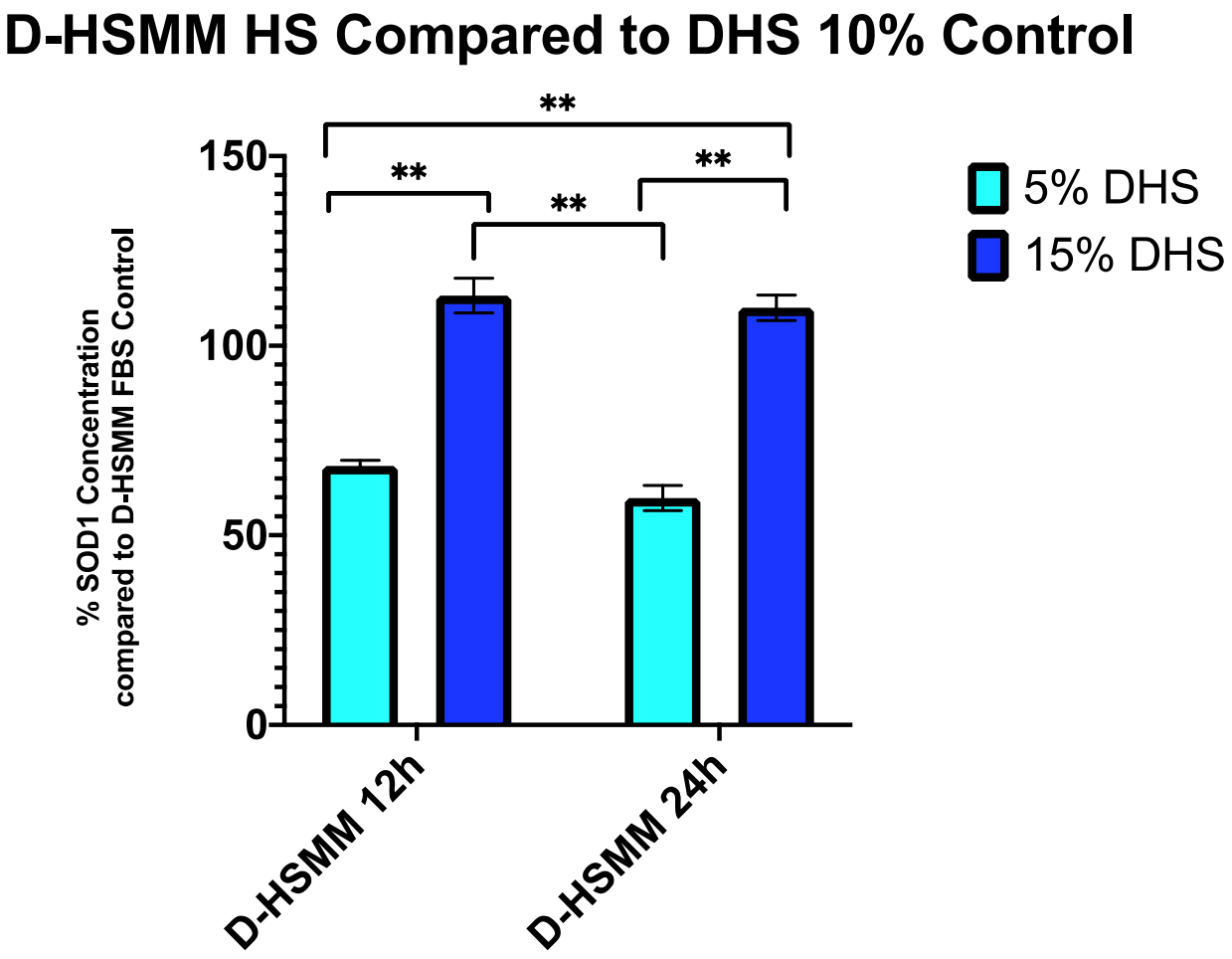

*Figure 22: Normalized SOD1 values of 12 vs 24h D-HSMM DHS compared to D-HSMM 10% DHS control. Alpha=0.05. *= p-value<0.05, **=p-value<0.01 ***=p-value <0.001.*

Source of Variation	% of total variation	P value	P value summary
Interaction	0.2997	0.4735	ns
Time	1.459	0.1561	ns
Treatment Concentration	96.32	0.0001	***

*Table 35: ANOVA results of 12 vs 24h D-HSMM DHS compared to D-HSMM 10% DHS control. Alpha=0.05. *= p-value<0.05, **=p-value<0.01 ***=p-value <0.001.*

4.5.3 TUMOR NECROSIS FACTOR ALPHA

Tumor necrosis factor alpha levels were normalized against the 10% FBS D-HSMM and are represented in figures 23-26 and tables 36-39. Treatment concentration had a significant effect on D-HSMM FBS model (p=0.007) (table 37) and also HSMM HS model (p=0.0124) (table 38).

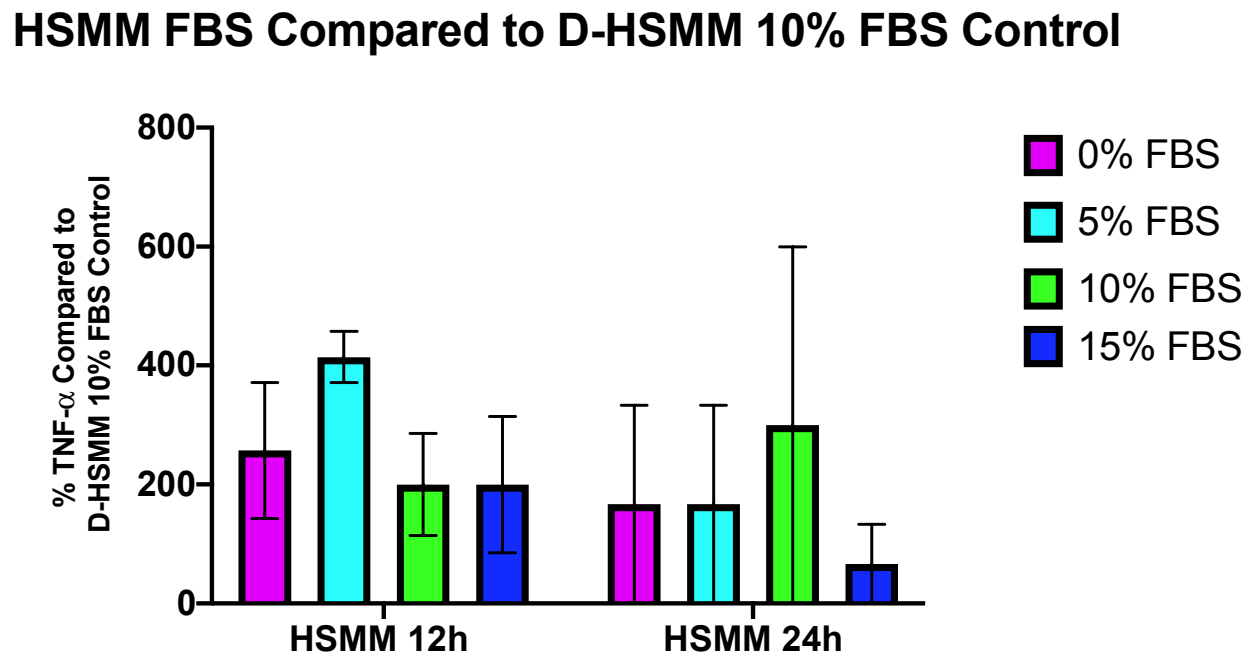

*Figure 23: Normalized TNF-α values of 12 vs 24h HSMM FBS compared to D-HSMM 10% FBS control. Alpha=0.05. *= p-value<0.05, **=p-value<0.01 ***=p-value <0.001.*

Source of Variation	% of total variation	P value	P value summary
Interaction	12.04	0.7231	ns
Time	6.612	0.4133	ns
Treatment Concentration	10.3	0.7658	ns

*Table 36: ANOVA results of 12 vs 24h HSMM FBS compared to D-HSMM 10% FBS control. Alpha=0.05. *= p-value<0.05, **=p-value<0.01 ***=p-value <0.001.*

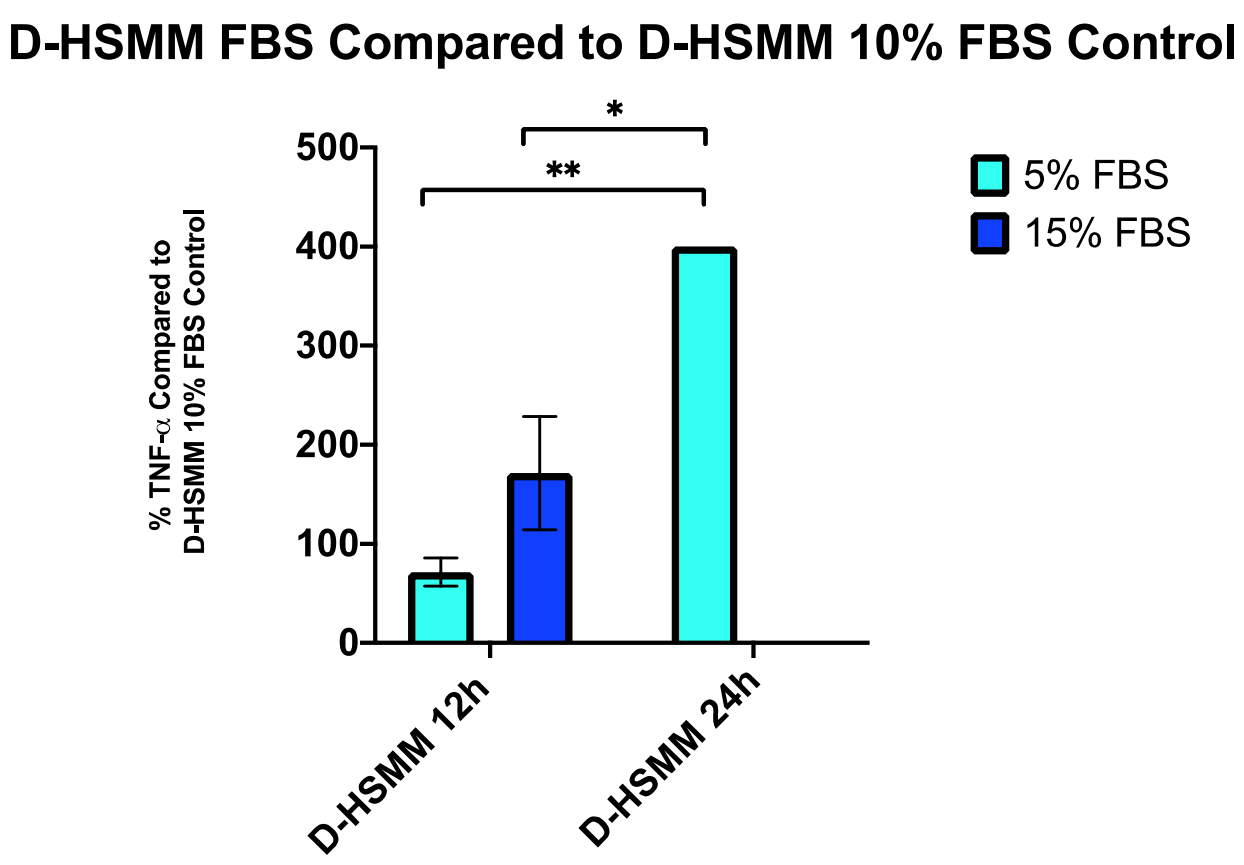

*Figure 24: Normalized TNF-α values of 12 vs 24h D-HSMM FBS compared to D-HSMM 10% FBS control. Alpha=0.05. *= p-value<0.05, **=p-value<0.01 ***=p-value <0.001. No bar present in the 24h 15% indicates no signal from assay.*

Source of Variation	% of total variation	P value	P value summary
Interaction	66.04	0.0011	**
Time	6.523	0.0559	ns
Treatment Concentration	23.77	0.007	**

*Table 37: ANOVA results of 12 vs 24h D-HSMM FBS compared to D-HSMM 10% FBS control. Alpha=0.05. *= p-value<0.05, **=p-value<0.01 ***=p-value <0.001.*

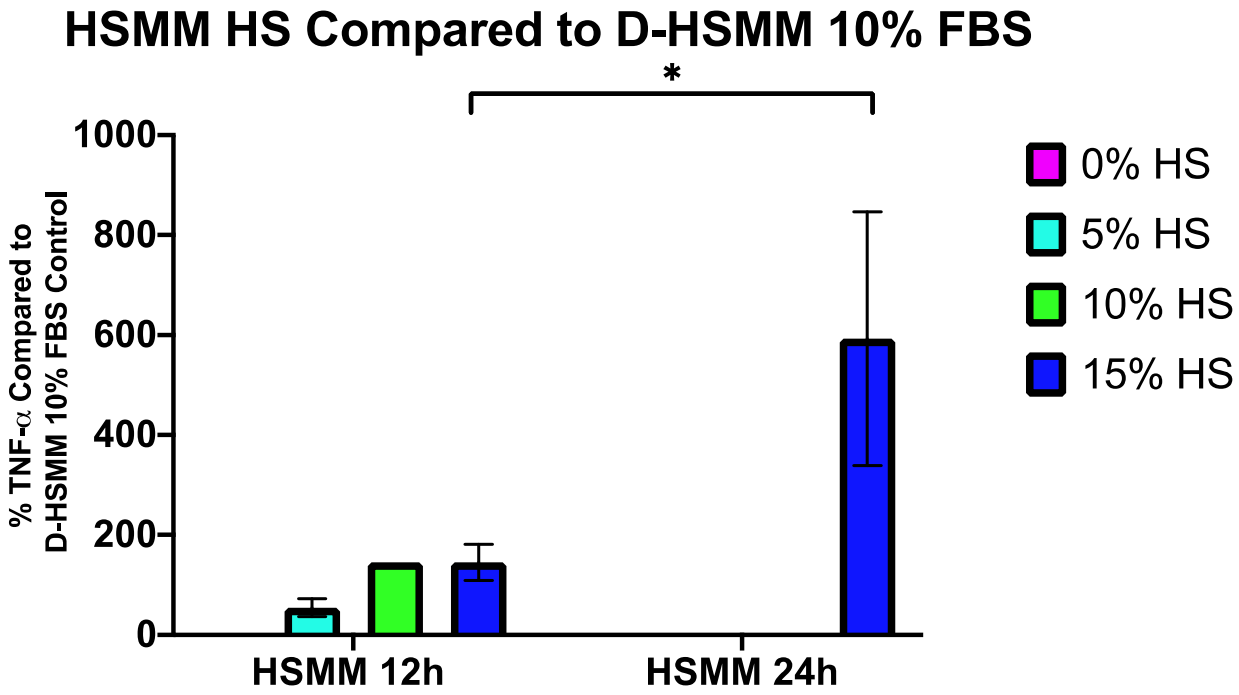

*Figure 25: Normalized TNF-α values of 12 vs 24h HSMM HS compared to D-HSMM 10% FBS control. Alpha=0.05. *= p-value<0.05, **=p-value<0.01 ***=p-value <0.001. No bar present in the 12h 0%, 24h 0%, 24h 5%, and 24h 10% indicates no signal from assay.*

Source of Variation	% of total variation	P value	P value summary
Interaction	29.62	0.0462	*
Time	2.179	0.3633	ns
Treatment Concentration	49.44	0.0124	*

*Table 38: ANOVA results of 12 vs 24h HSMM HS compared to D-HSMM 10% FBS control. Alpha=0.05. *= p-value<0.05, **=p-value<0.01 ***=p-value <0.001.*

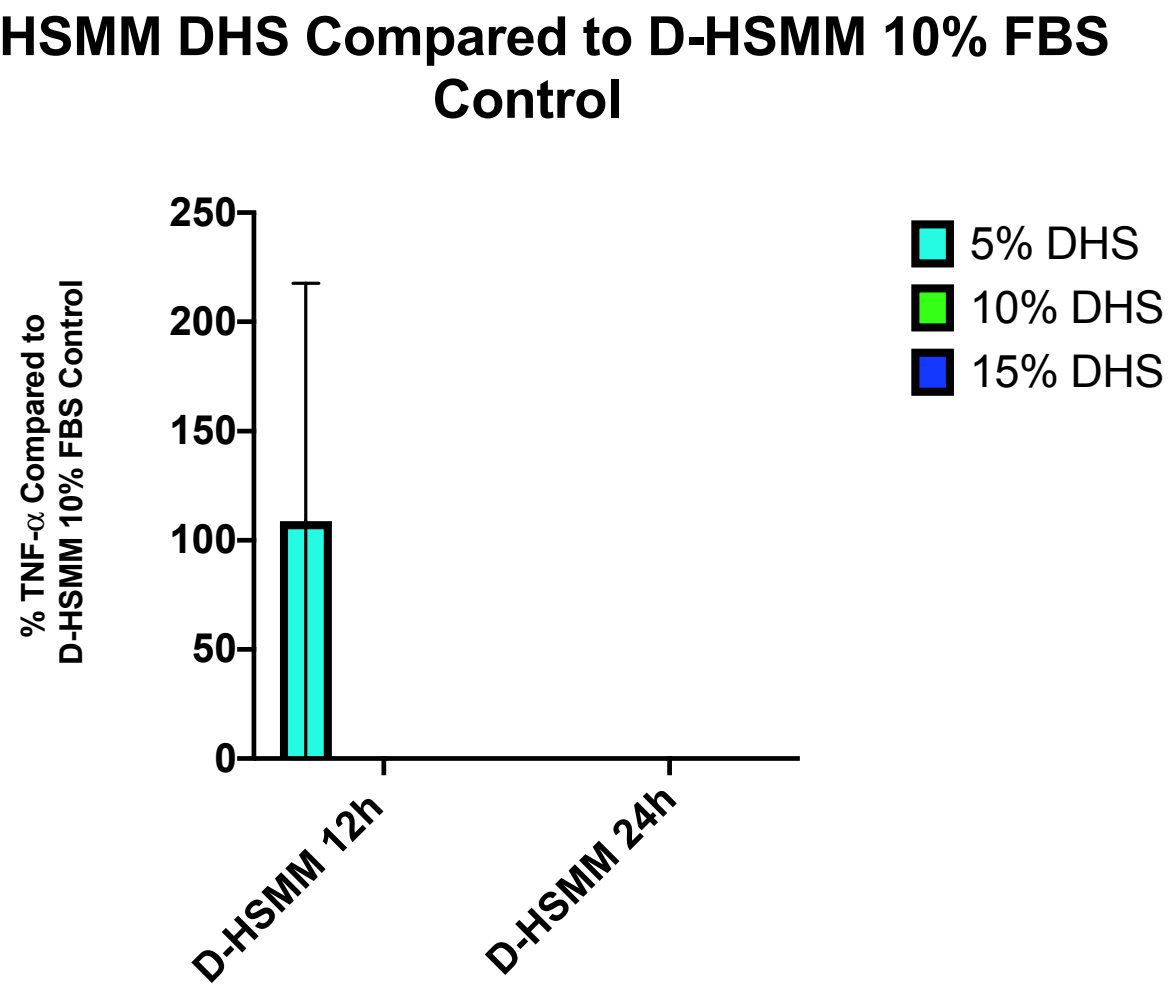

*Figure 26: Normalized TNF-α values of 12 vs 24h D-HSMM HS compared to D-HSMM 10% FBS control. Alpha=0.05. *= p-value<0.05, **=p-value<0.01 ***=p-value <0.001. No bar present in the 12h 10%, 12h 15%, 24h 5%, 24h 10% and 24h 15% indicates no signal from assay.*

Source of Variation	% of total variation	P value	P value summary
Interaction	18.18	0.4219	ns
Time	9.091	0.3559	ns
Treatment Concentration	18.18	0.4219	ns

*Table 39: ANOVA results of 12 vs 24h D-HSMM HS compared to D-HSMM 10% FBS control. Alpha=0.05. *= p-value<0.05, **=p-value<0.01 ***=p-value <0.001.*

4.6 PCR ANALYSIS AND GENE EXPRESSION

Table 40 represents the fold change in gene expression for each gene measured at each treatment concentration. The dash symbolizes inconclusive data. Unfortunately, values from 5% HSMM cells were corrupted due to incorrect cycling conditions and were not reported. Interestingly, the highest fold changes were seen in HSMM cells in the 15% serum, representing an over nutrition state. A 1.378-fold change was seen in AKT2, and a 1.18-fold change was observed in MSTN. There was also an observed 0.081-fold increase in FBXO32 (Atrogin-1) expression in 5% D-HSMM sample.

	HSMM		**D-HSMM**		
Gene	**10% HS**	**15% HS**	**5% DHS**	**10% DHS**	**15% DHS**
18S	-	-	-	-	-
ACTA1	-	-	-	-	-
AKT1	1	0.724	0.04	0.027	0.064
AKT2	1	1.378	0.031	0.024	0.064
CAPN2	1	0.865	0.031	0.026	0.06
FBXO32	1	0.125	0.081	0.092	0.206
FOXO1	1	0.369	0.049	0.033	0.133
FOXO3	-	-	-	-	-
IGF1	-	-	-	-	-
IL6	1	-	0.011	0.01	0.027
IL1B	-	-	-	-	-
MSTN	1	1.187	0.049	0.093	0.232
PRKAA1	1	0.563	0.022	0.033	0.062
RPS6KB1	1	-	0.016	0.028	0.081
TNF	-	-	-	-	-

Table 40: Fold change in gene expression for each gene.

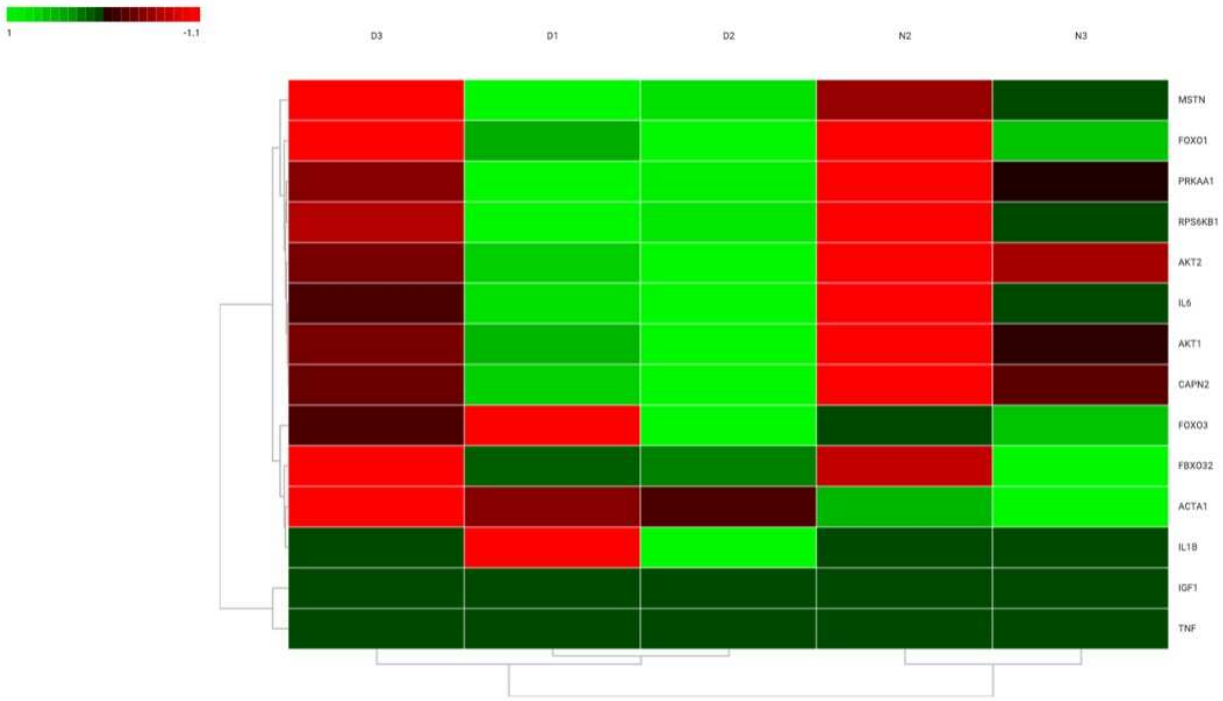

Figure 27: Heat map of genes at each cell concentration. N2 and N3 represent HSMM 10% HS and 15%, respectively. D1, D2, and D3 represent D-HSMM 5% DHS, 10% DHS, and 15% DHS, respectively.

5. DISCUSSION

5.1 CELL VIABILITY AND SERUM CONCENTRATION

Skeletal muscle mass reduction is a common symptom of Type 2 diabetics, especially in aging populations[50]. It is imperative that the risks of T2D and aging be mitigated, and many have attempted to combat these issues through nutrition. While fasting regimens may have positive results on weight loss, the harms to other body systems, including muscle, are still unclear. Intermittent fasting has also been associated with a twofold increase in the chance of a hypoglycemic event in Type 2 diabetic humans on fasting days[51]. Hypoglycemia can lead to many health issues, including sarcopenia and frailty in older patients[52]. Similarly,

extended periods of hyperglycemia, a common effect of T2D, can cause muscle atrophy and loss of muscle mass[53,54]. While overnutrition can cause insulin resistance[55], undernutrition may also have harmful effects.

This study aimed to replicate over nutrition and fasting conditions in skeletal muscle myoblasts. The molecular mechanisms present at the cellular level can indicate how varying nutritional levels may affect whole body systems. Standard cell culture protocol calls for cell culture media to remain at 10% FBS for optimal growth. A negative control group was plated with 0% serum. As expected, the cell viability and density of the negative control was very low compared to the other treatment groups. To simulate a fast, one treatment group was plated with 5% serum. To simulate overnutrition, cells were plated with 15% serum.

The normalized data revealed that treatment concentration may have an effect on cell viability in both FBS ($p=0.0045$) and HS ($p<0.0001$) HSMM models. As time progresses from 12 to 24 hours, cell viability also appears to increase in both the FBS ($p=0.0228$) and HS ($p<0.0001$) HSMM model. The significant increase seen in the HS model could be due to healthy exercised cells being less susceptible to muscle wasting, seen in the lean body mass of elderly patients that undergo progressive resistance training[56]. Other confounding variables, like differing concentrations of total protein, albumin, and estradiol[58] may also account for differences in human serum cell culture models compared to cells cultured with bovine products. These differences may account for the increase seen in this model. As time progresses from 12 to 24 hours in the D-HSMM cells plated with DHS, there was an increase in cell viability ($p=0.0026$). The D-HSMM DHS model depicts the 5% DHS as the lowest viability in both 12 and 24 hours. This suggests that diabetic muscle cells may be more susceptible to muscle atrophy when placed in nutrient deficient conditions, as it is similar to a hypoglycemic event, as seen in

rabbits induced by experimental hypoglycemia[59]. When data is normalized against the diabetic control, similar effects of time and treatment concentration are observed in both HSMM and D-HSMM models. Overall, viability for each treatment group reflected no definite pattern, but individual values indicate instances of potential muscle cell atrophy.

5.2 OXIDATIVE STRESS AND SUPEROXIDE DISMUTASE 1

Oxidative stress is closely linked to impaired metabolic homeostasis and increased inflammation, which plays a significant role in the development of insulin resistance seen in T2D[28,29,32]. Metabolic abnormalities caused by T2D cause mitochondrial superoxide overproduction which results in cellular damage[60]. Further, oxidative stress caused by hyperglycemia impairs the prooxidant/antioxidant balance, which increases free radicals. This imbalance has also shown to impair muscle repair in diabetic rat models[61].

Superoxide, a harmful ROS primarily produced by oxygen metabolism, is typically mitigated by superoxide dismutase 1. SOD1 is an antioxidant enzyme that converts superoxide into molecular oxygen and hydrogen peroxide, which are less toxic compounds. In both HSMM and D-HSMM models that were plated with pooled HS, we observed a stepwise increase in the concentration of SOD1 in serum in both 12- and 24-hour treatment groups. We hypothesize that the increasing values seen from 5%-15% serum are due to exogenous SOD1 that was present at the time of plating. This could be due to differences seen in fluorescence emission from human serum compared with bovine products[62]. Due to limitations on this study, we were unable to measure the presence and rate of decay of enzymes already present in the pooled human serum. When analyzing the normalized levels of SOD1 in HSMM FBS, treatment concentration accounts for 39.84% of variation in this model. While this effect is not statistically significant ($p=0.0787$), it may suggest that the increase in SOD1 from 12 to 24 hours in the 5% category

was caused by the nutritionally scarce environment. A previous study also suggested that food deprivation increases oxidative stress in rat liver by increasing free radical generation in the mitochondria[63]. Higher levels of SOD1 were seen in all treatment concentrations in the D-HSMM FBS model compared to the HSMM FBS model. This may be because type 2 diabetes and other metabolic diseases are associated with higher levels of ROS. Increasing glucose intake has also been shown to induce ROS formation and shorten the lifespan of *C. elegans*[64].

Similar patterns were noted with data normalized against D-HSMM 10% models. Interestingly, when the diabetic control was used, the effect of time and treatment concentration became significant in the HSMM FBS model ($p=0.001$ and $p<0.0001$, respectively). The individual effect between 5% FBS from 12 to 24 hours changed from $p=0.07$ when normalized against the HSMM model to $p=0.054$ when normalized against the D-HSMM model, indicating that the nutritionally scarce environment may influence SOD1 levels. Stepwise increases were also observed in human serum models. No significant differences were observed in D-HSMM FBS model when normalized against D-HSMM 10% FBS. This model depicts an increase in SOD1 5% from 12 to 24 hours, although this effect was insignificant.

5.3 TUMOR NECROSIS FACTOR ALPHA

This study aimed to determine if nutritional serum concentration had an effect on TNF-α concentration in serum after 12 and 24 hours, and if this effect was exacerbated in D-HSMM cells. The data suggests that there is a significant effect of time on HSMM cells plated with FBS ($p=0.0211$). Interestingly, the highest incidence of TNF- α was seen in 5% FBS, but then decreased after 24 hours. As time progresses, the data reflects a reduction in TNF-α concentration. This could be due to reduced basal cytokine expression, which has been seen in white adipose tissue of rats fasted for 24 hours[65]. Conversely, D-HSMM cells plated with 5%

FBS indicate an increase in TNF-α levels from 12 to 24 hours, although this was not significant. This could point to an occurrence of D-HSMM cells increasing inflammation in nutrient poor environments. In HSMM cells plated with 15% HS, there was a slight increase seen from 12 to 24 hours. This could indicate that hyperglycemic environment may also cause an upregulation in TNF-α causing atrophy. Existing data suggests that TNF-α stimulates muscle catabolism by activating the ubiquitin/proteasome pathway[66]. In D-HSMM cells plated with DHS, however, there was virtually no indication of TNF-α activity. This is contrary to most literature, as serum TNF-α is largely associated with insulin resistance seen in type 2 diabetes[67]. A longer and more extensive fast might produce a stronger TNF-α signal.

When TNF-α values were normalized against the D-HSMM control, the highest value was seen in HSMM 5% FBS at 12 hours but was also seen to decrease at 24 hours. In the D-HSMM FBS model normalized against D-HSMM 10% FBS, a significant increase in TNF-α was seen in 5% FBS from 12 to 24 hours ($p=0.0048$). This value suggests that the nutritionally scarce environment increases inflammatory processes, which increases TNF-α levels. This was not seen in the HS/DHS models, as there was low signal of TNF-α in serum compared to the standard curve, likely out of detection range. Overall, the results may suggest presence of inflammation due to nutritional stress, but there are no definite patterns that can be reported.

5.4 GENE EXPRESSION

An array of genes was qualitatively analyzed from the 24-hour human serum treatment groups. Human serum concentrations 5%, 10%, and 15% were analyzed for both HSMM and D-HSMM cells. Interestingly, the highest fold-changes seen were in the cells grown in a nutrient excess state. Specifically, the 1.187-fold increase in Myostatin seen in 15% HSMM cells. Myostatin is a negative regulator of muscular growth, and an upregulation indicates that cells are

in a stressed state and are atrophying. A 1.378-fold increase was also observed in AKT2, one of the highest AKT isoform transcripts seen in muscle[58]. AKT2, a serine/threonine-protein kinase, is responsible for activating mTOR, a positive regulator of protein synthesis. The presence of both Myostatin, a negative regulator of protein synthesis, and AKT2, a positive regulator of protein synthesis, is paradoxical. A possible explanation for this is that the high amount of glucose could be causing disruptions in metabolic processes, which is seen in overweight humans who are diagnosed with metabolic syndrome[69]. A 0.865-fold change in Calpain-2 was also observed in this sample. The Calpain family of proteins mediate protein degradation. With the observed upregulation of Calpain-2 and Myostatin, there is evidence of protein degradation in a nutrient excess state.

A 0.081-fold change in atrophy biomarker FBXO32 (Atrogin-1) was observed in D-HSMM cells in a 5% nutrient poor state. Atrogin-1 is a E3 ubiquitin ligase, and its presence indicates that the ubiquitin proteasomal pathway was activated causing proteolytic activity. Atrogin-1 is specifically expressed in skeletal muscle and directs the polyubiquitination of proteins and targets them for proteolysis, and is also induced by Myostatin[70]. Although Atrogin-1 was not present in serum, its presence in the RNA indicates that the muscles were being degraded.

While this data is qualitative, it indicates possible areas for further research regarding muscle atrophy. However, it is important to note the paradoxical effect that was observed with AKT2. While cell degradation pathways may be activated, separate cell proliferation may also be present. These variables should be taken into account when performing further research.

5.5 SUMMARY

The data reported in this study indicate changes in muscle cell function that will require further research. While some of the data may be inconclusive, other significant patterns indicate that nutrient poor fasting conditions, and also over saturated, nutrient rich conditions can have deleterious effects on muscle cells. This is reflected by an increase in oxidative stress marker SOD1 in cells plated in nutrient poor conditions. An increase in pro-inflammatory marker TNF-α is also seen in both HSMM and D-HSMM cells plated in nutrient poor FBS, indicating muscle stress and potential atrophy. The gene expression analysis also reflected an upregulation in several atrophy biomarkers in both D-HSMM and HSMM cells in nutrient poor and rich conditions. The 1.187-fold increase in Myostatin, a negative regulator of muscle growth[71], seen in 15% DHS HSMM cells is also indicative of the harmful effects of overnutrition. Similarly, the 0.206-fold increase in atrophy gene FBXO32 (Atrogin-1) seen in 15% DHS D-HSMM reflects negative consequences of overnutrition. The 0.031-fold increase in Calpain-2 seen in 5% DHS D-HSMM cells indicates an increase in proteolytic activity. Calpain-2 has been shown to upregulate during starvation of rainbow trout[72], indicating that the activity of calpain-2 mobilizes muscle for an energy source in times of nutrient scarcity. This could be a possible explanation of the upregulation seen in the D-HSMM model. Although this was a qualitative assessment of genes, it should be utilized as a vehicle for further research into gene analysis and expression when exposed to varying nutrient concentrations. Overall, the results indicate that the different nutrient states have an effect on muscle, and these effects can be harmful.

The metabolic processes of human skeletal muscle are important indicators of potential whole system effects on muscle as an organ system. Nutrition is a vital aspect of human health and should be especially considered when dealing with diabetic and aging populations. When

studying nutrition, researchers tend to focus on the effects that happen to fat and adipose tissue, while disregarding potential harms that can happen to muscle.

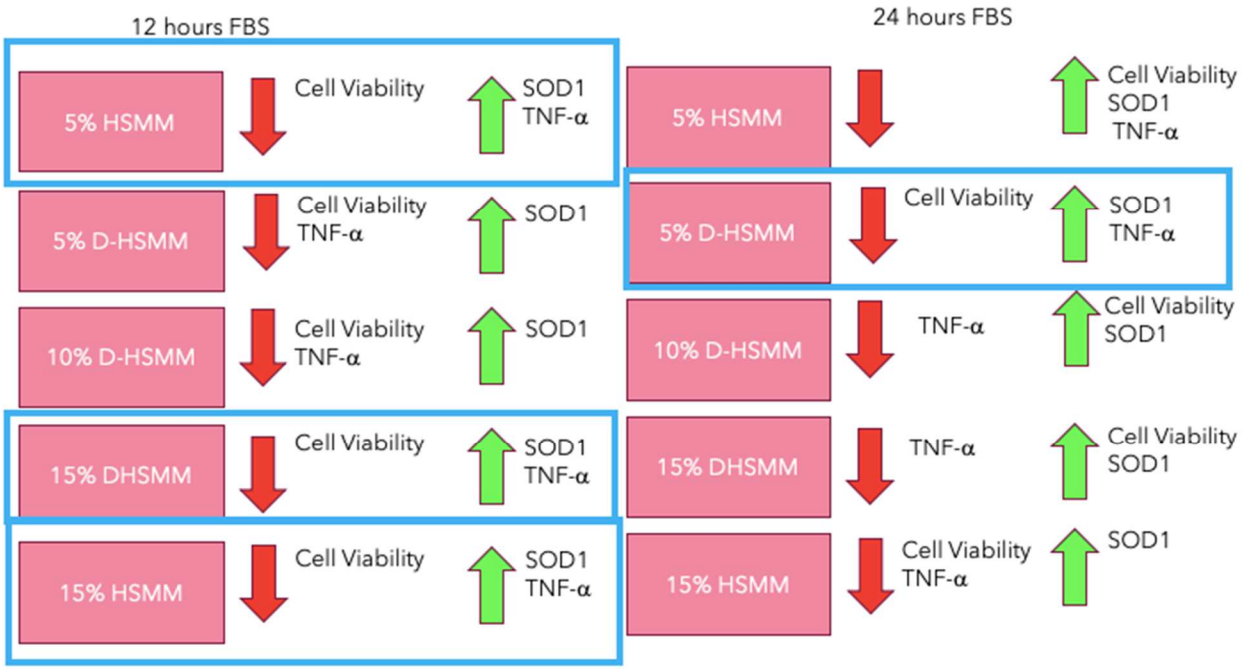

Figure 28: 12- and 24-hour D-HSMM and HSMMM FBS summary of results

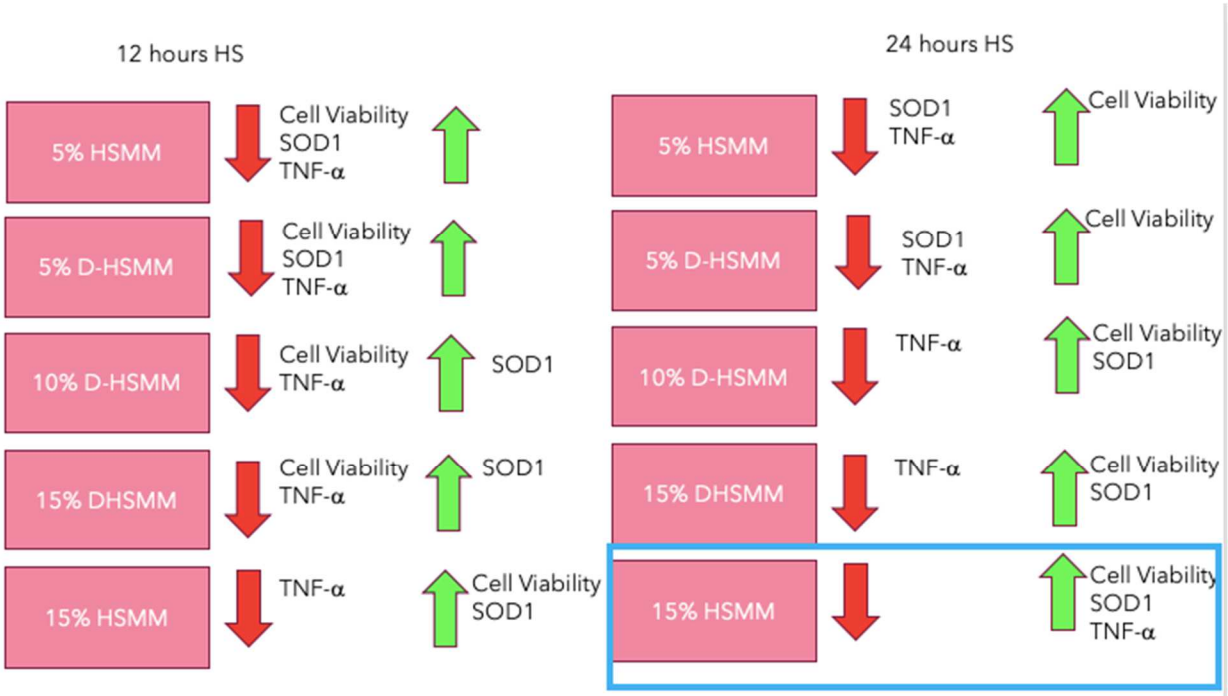

Figure 29: 12- and 24-hour D-HSMM and HSMMM HS/DHS summary of results

Figure 30: Gene expression summary

Recommendations for further study include: (1) quantitatively assessing gene expression in atrogenes following nutrient stress; (2) performing nutrient stress experiments at a more extensive range of treatment concentrations (i.e. 0%-10% serum); (3) performing nutrient stress experiments for longer time periods; (4) assessing the effect of "re-feeding" on muscle cells; and (5) assessing effects of fasting on muscle in a human model.

5. REFERENCES

1. Longo VD, Mattson MP. Fasting: Molecular Mechanisms and Clinical Applications. *Cell Metab*. 2014;19(2):181-192. doi:10.1016/j.cmet.2013.12.008

2. Gonidakis S, Finkel SE, Longo VD. Genome-wide screen identifies Escherichia coli TCA-cycle-related mutants with extended chronological lifespan dependent on acetate metabolism and the hypoxia-inducible transcription factor ArcA. *Aging Cell*. 2010;9(5):868-881. doi:10.1111/j.1474-9726.2010.00618.x

3. Lee GD, Wilson MA, Zhu M, et al. Dietary deprivation extends lifespan in Caenorhabditis elegans. *Aging Cell*. 2006;5(6):515-524. doi:10.1111/j.1474-9726.2006.00241.x

4. Brandhorst S, Choi IY, Wei M, et al. A Periodic Diet that Mimics Fasting Promotes Multi-System Regeneration, Enhanced Cognitive Performance, and Healthspan. *Cell Metab*. 2015;22(1):86-99. doi:10.1016/j.cmet.2015.05.012

5. Filomeni G, De Zio D, Cecconi F. Oxidative stress and autophagy: the clash between damage and metabolic needs. *Cell Death Differ*. 2015;22(3):377-388. doi:10.1038/cdd.2014.150

6. Sacheck JM, Ohtsuka A, McLary SC, Goldberg AL. IGF-I stimulates muscle growth by suppressing protein breakdown and expression of atrophy-related ubiquitin ligases, atrogin-1 and MuRF1. *Am J Physiol-Endocrinol Metab*. 2004;287(4):E591-E601. doi:10.1152/ajpendo.00073.2004

7. Bagherniya M, Butler AE, Barreto GE, Sahebkar A. The effect of fasting or calorie restriction on autophagy induction: A review of the literature. *Ageing Res Rev*. 2018;47:183-197. doi:10.1016/j.arr.2018.08.004

8. Wu WKK, Coffelt SB, Cho CH, et al. The autophagic paradox in cancer therapy. *Oncogene*. 2012;31(8):939-953. doi:10.1038/onc.2011.295

9. Kuo H-P, Lee D-F, Chen C-T, et al. ARD1 Stabilization of TSC2 Suppresses Tumorigenesis Through the mTOR Signaling Pathway. *Sci Signal*. 2010;3(108):ra9. doi:10.1126/scisignal.2000590

10. Wang J, Whiteman MW, Lian H, et al. A Non-canonical MEK/ERK Signaling Pathway Regulates Autophagy via Regulating Beclin 1. *J Biol Chem*. 2009;284(32):21412-21424. doi:10.1074/jbc.M109.026013

11. Heilbronn LK, Smith SR, Martin CK, Anton SD, Ravussin E. Alternate-day fasting in nonobese subjects: effects on body weight, body composition, and energy metabolism. *Am J Clin Nutr*. 2005;81(1):69-73. doi:10.1093/ajcn/81.1.69

12. Schaumberg K, Anderson DA, Anderson LM, Reilly EE, Gorrell S. Dietary restraint: what's the harm? A review of the relationship between dietary restraint, weight trajectory and the development of eating pathology. *Clin Obes*. 2016;6(2):89-100. doi:10.1111/cob.12134

13. Heilbronn LK, Civitarese AE, Bogacka I, Smith SR, Hulver M, Ravussin E. Glucose Tolerance and Skeletal Muscle Gene Expression in Response to Alternate Day Fasting. *Obes Res*. 2005;13(3):574-581. doi:10.1038/oby.2005.61

14. Soeters MR, Lammers NM, Dubbelhuis PF, et al. Intermittent fasting does not affect whole-body glucose, lipid, or protein metabolism. *Am J Clin Nutr*. 2009;90(5):1244-1251. doi:10.3945/ajcn.2008.27327

15. Catenacci VA, Pan Z, Ostendorf D, et al. A randomized pilot study comparing zero-calorie alternate-day fasting to daily caloric restriction in adults with obesity: Alternate-Day Fasting Versus Caloric Restriction. *Obesity*. 2016;24(9):1874-1883. doi:10.1002/oby.21581

16. Lecker SH, Goldberg AL, Mitch WE. Protein Degradation by the Ubiquitin–Proteasome Pathway in Normal and Disease States. *J Am Soc Nephrol*. 2006;17(7):1807-1819. doi:10.1681/ASN.2006010083

17. Lum JJ, DeBerardinis RJ, Thompson CB. Autophagy in metazoans: cell survival in the land of plenty. *Nat Rev Mol Cell Biol*. 2005;6(6):439-448. doi:10.1038/nrm1660

18. Tran H, Brunet A, Griffith EC, Greenberg ME. The many forks in FOXO's road. *Sci STKE Signal Transduct Knowl Environ*. 2003;2003(172):RE5. doi:10.1126/stke.2003.172.re5

19. Accili D, Arden KC. FoxOs at the crossroads of cellular metabolism, differentiation, and transformation. *Cell*. 2004;117(4):421-426.

20. Sandri M, Sandri C, Gilbert A, et al. Foxo Transcription Factors Induce the Atrophy-Related Ubiquitin Ligase Atrogin-1 and Cause Skeletal Muscle Atrophy. *Cell*. 2004;117(3):399-412. doi:10.1016/S0092-8674(04)00400-3

21. Cong H, Sun L, Liu C, Tien P. Inhibition of atrogin-1/MAFbx expression by adenovirus-delivered small hairpin RNAs attenuates muscle atrophy in fasting mice. *Hum Gene Ther*. 2011;22(3):313-324. doi:10.1089/hum.2010.057

22. Ogata T, Oishi Y, Higuchi M, Muraoka I. Fasting-related autophagic response in slow- and fast-twitch skeletal muscle. *Biochem Biophys Res Commun*. 2010;394(1):136-140. doi:10.1016/j.bbrc.2010.02.130

23. Bodine SC, Latres E, Baumhueter S, et al. Identification of ubiquitin ligases required for skeletal muscle atrophy. *Science*. 2001;294(5547):1704-1708. doi:10.1126/science.1065874

24. Gomes MD, Lecker SH, Jagoe RT, Navon A, Goldberg AL. Atrogin-1, a muscle-specific F-box protein highly expressed during muscle atrophy. *Proc Natl Acad Sci*. 2001;98(25):14440-14445. doi:10.1073/pnas.251541198

25. Mammucari C, Milan G, Romanello V, et al. FoxO3 Controls Autophagy in Skeletal Muscle In Vivo. *Cell Metab*. 2007;6(6):458-471. doi:10.1016/j.cmet.2007.11.001

26. Cohen S, Nathan JA, Goldberg AL. Muscle wasting in disease: molecular mechanisms and promising therapies. *Nat Rev Drug Discov*. 2015;14(1):58-74. doi:10.1038/nrd4467

27. American Diabetes Association. Diagnosis and Classification of Diabetes Mellitus. *Diabetes Care*. 2010;33(Supplement_1):S62-S69. doi:10.2337/dc10-S062

28. Rehman K, Akash MSH. Mechanism of Generation of Oxidative Stress and Pathophysiology of Type 2 Diabetes Mellitus: How Are They Interlinked?: O XIDATIVE S TRESS AND D IABETES M ELLITUS. *J Cell Biochem*. 2017;118(11):3577-3585. doi:10.1002/jcb.26097

29. Bayir A, Sirkecioglu AN, Bayir M, Haliloglu HI, Kocaman EM, Aras NM. Metabolic responses to prolonged starvation, food restriction, and refeeding in the brown trout, Salmo trutta: Oxidative stress and antioxidant defenses. *Comp Biochem Physiol B Biochem Mol Biol*. 2011;159(4):191-196. doi:10.1016/j.cbpb.2011.04.008

30. Podbregar M, Lainscak M, Prelovsek O, Mars T. Cytokine Response of Cultured Skeletal Muscle Cells Stimulated with Proinflammatory Factors Depends on Differentiation Stage. *Sci World J*. 2013;2013:1-8. doi:10.1155/2013/617170

31. Zhou J, Liu B, Liang C, Li Y, Song Y-H. Cytokine Signaling in Skeletal Muscle Wasting. *Trends Endocrinol Metab*. 2016;27(5):335-347. doi:10.1016/j.tem.2016.03.002

32. Asmat U, Abad K, Ismail K. Diabetes mellitus and oxidative stress—A concise review. *Saudi Pharm J*. 2016;24(5):547-553. doi:10.1016/j.jsps.2015.03.013

33. Ahima RS, Park H-K. Connecting Myokines and Metabolism. *Endocrinol Metab*. 2015;30(3):235. doi:10.3803/EnM.2015.30.3.235

34. Saghizadeh M, Ong JM, Garvey WT, Henry RR, Kern PA. The expression of TNF alpha by human muscle. Relationship to insulin resistance. *J Clin Invest*. 1996;97(4):1111-1116. doi:10.1172/JCI118504

35. Eckel J. Myokines in metabolic homeostasis and diabetes. *Diabetologia*. 2019;62(9):1523-1528. doi:10.1007/s00125-019-4927-9

36. Handschin C, Spiegelman BM. The role of exercise and PGC1α in inflammation and chronic disease. *Nature*. 2008;454(7203):463-469. doi:10.1038/nature07206

37. Bouzakri K, Zierath JR. MAP4K4 Gene Silencing in Human Skeletal Muscle Prevents Tumor Necrosis Factor-α-induced Insulin Resistance. *J Biol Chem*. 2007;282(11):7783-7789. doi:10.1074/jbc.M608602200

38. Plomgaard P, Bouzakri K, Krogh-Madsen R, Mittendorfer B, Zierath JR, Pedersen BK. Tumor Necrosis Factor-α Induces Skeletal Muscle Insulin Resistance in Healthy Human Subjects via Inhibition of Akt Substrate 160 Phosphorylation. *Diabetes*. 2005;54(10):2939-2945. doi:10.2337/diabetes.54.10.2939

39. Pedersen BK. Exercise-induced myokines and their role in chronic diseases. *Brain Behav Immun*. 2011;25(5):811-816. doi:10.1016/j.bbi.2011.02.010

40. Lang CH, Frost RA, Nairn AC, MacLean DA, Vary TC. TNF-α impairs heart and skeletal muscle protein synthesis by altering translation initiation. *Am J Physiol-Endocrinol Metab*. 2002;282(2):E336-E347. doi:10.1152/ajpendo.00366.2001

41. Franceschi C, Garagnani P, Parini P, Giuliani C, Santoro A. Inflammaging: a new immune–metabolic viewpoint for age-related diseases. *Nat Rev Endocrinol*. 2018;14(10):576-590. doi:10.1038/s41574-018-0059-4

42. Pirkmajer S, Chibalin AV. Serum starvation: *caveat emptor*. *Am J Physiol-Cell Physiol*. 2011;301(2):C272-C279. doi:10.1152/ajpcell.00091.2011

43. Mbeunkui F, Fodstad O, Pannell LK. Secretory protein enrichment and analysis: an optimized approach applied on cancer cell lines using 2D LC-MS/MS. *J Proteome Res*. 2006;5(4):899-906. doi:10.1021/pr050375p

44. Bouzakri K, Zachrisson A, Al-Khalili L, et al. siRNA-based gene silencing reveals specialized roles of IRS-1/Akt2 and IRS-2/Akt1 in glucose and lipid metabolism in human skeletal muscle. *Cell Metab*. 2006;4(1):89-96. doi:10.1016/j.cmet.2006.04.008

45. Lambert K, Pirt SJ. Growth of human diploid cells (strain MRC-5) in defined medium; replacement of serum by a fraction of serum ultrafiltrate. *J Cell Sci*. Published online 1979.

46. Colzani M, Waridel P, Laurent J, Faes E, Rüegg C, Quadroni M. Metabolic Labeling and Protein Linearization Technology Allow the Study of Proteins Secreted by Cultured Cells in Serum-Containing Media. doi:10.1021/pr900476b

47. Tateishi K, Ando W, Higuchi C, et al. Comparison of human serum with fetal bovine serum for expansion and differentiation of human synovial MSC: potential feasibility for clinical applications. *Cell Transplant*. 2008;17(5):549-557.

48. Ali F, Aziz F, Wajid N. Effect of type 2 diabetic serum on the behavior of Wharton's jelly-derived mesenchymal stem cells in vitro. *Chronic Dis Transl Med*. 2017;3(2):105-111. doi:10.1016/j.cdtm.2017.02.006

49. Nakai N, Kitai S, Iida N, et al. Induction of Autophagy and Changes in Cellular Metabolism in Glucose Starved C2C12 Myotubes. *J Nutr Sci Vitaminol (Tokyo)*. 2020;66(1):41-47. doi:10.3177/jnsv.66.41

50. Larson AA, Syverud BC, Florida SE, Rodriguez BL, Pantelic MN, Larkin LM. Effects of dexamethasone dose and timing on tissue-engineered skeletal muscle units. *Cells Tissues Organs*. 2018;205(4):197-207. doi:10.1159/000490884

51. Kim K-S, Park K-S, Kim M-J, Kim S-K, Cho Y-W, Park SW. Type 2 diabetes is associated with low muscle mass in older adults. *Geriatr Gerontol Int*. 2014;14(S1):115-121. doi:10.1111/ggi.12189

52. Corley BT, Carroll RW, Hall RM, Weatherall M, Parry-Strong A, Krebs JD. Intermittent fasting in Type 2 diabetes mellitus and the risk of hypoglycaemia: a randomized controlled trial. *Diabet Med J Br Diabet Assoc*. 2018;35(5):588-594. doi:10.1111/dme.13595

53. Umegaki H. Sarcopenia and frailty in older patients with diabetes mellitus. *Geriatr Gerontol Int*. 2016;16(3):293-299. doi:10.1111/ggi.12688

54. Hirata Y, Nomura K, Senga Y, et al. Hyperglycemia induces skeletal muscle atrophy via a WWP1/KLF15 axis. *JCI Insight*. 2019;4(4). doi:10.1172/jci.insight.124952

55. Kalyani RR, Metter EJ, Egan J, Golden SH, Ferrucci L. Hyperglycemia Predicts Persistently Lower Muscle Strength With Aging. *Diabetes Care*. 2015;38(1):82-90. doi:10.2337/dc14-1166

56. Wang X, Hu Z, Hu J, Du J, Mitch WE. Insulin Resistance Accelerates Muscle Protein Degradation: Activation of the Ubiquitin-Proteasome Pathway by Defects in Muscle Cell Signaling. *Endocrinology*. 2006;147(9):4160-4168. doi:10.1210/en.2006-0251

57. Fielding RA. The role of progressive resistance training and nutrition in the preservation of lean body mass in the elderly. *J Am Coll Nutr*. 1995;14(6):587-594. doi:10.1080/07315724.1995.10718547

58. Heger JI, Froehlich K, Pastuschek J, et al. Human serum alters cell culture behavior and improves spheroid formation in comparison to fetal bovine serum. *Exp Cell Res*. 2018;365(1):57-65. doi:10.1016/j.yexcr.2018.02.017

59. Jiang ZL, Harada T, Yokokawa M, Kohzuki M, Sato T. Muscle damage induced by experimental hypoglycemia. *Metabolism*. 1998;47(12):1472-1476. doi:10.1016/s0026-0495(98)90072-5

60. Giacco F, Brownlee M. Oxidative Stress and Diabetic Complications. Schmidt AM, ed. *Circ Res*. 2010;107(9):1058-1070. doi:10.1161/CIRCRESAHA.110.223545

61. Aragno M, Mastrocola R, Catalano MG, Brignardello E, Danni O, Boccuzzi G. Oxidative Stress Impairs Skeletal Muscle Repair in Diabetic Rats. *Diabetes*. 2004;53(4):1082-1088. doi:10.2337/diabetes.53.4.1082

62. Steinhardt J, Krijn J, Leidy JG. Differences between bovine and human serum albumins. Binding isotherms, optical rotatory dispersion, viscosity, hydrogen ion titration, and fluorescence effects. doi:10.1021/bi00798a001

63. Sorensen M, Sanz A, Gómez J, et al. Effects of fasting on oxidative stress in rat liver mitochondria. *Free Radic Res*. 2006;40(4):339-347. doi:10.1080/10715760500250182

64. Lee S-J, Murphy CT, Kenyon C. Glucose shortens the life span of C. elegans by downregulating DAF-16/FOXO activity and aquaporin gene expression. *Cell Metab*. 2009;10(5):379-391. doi:10.1016/j.cmet.2009.10.003

65. Speaker KJ, Paton MM, Cox SS, Fleshner M. A Single Bout of Fasting (24 h) Reduces Basal Cytokine Expression and Minimally Impacts the Sterile Inflammatory Response in the White Adipose Tissue of Normal Weight F344 Rats. Mediators of Inflammation. doi:https://doi.org/10.1155/2016/1698071

66. Reid MB, Li Y-P. Tumor necrosis factor-α and muscle wasting: a cellular perspective. *Respir Res*. 2001;2(5):269-272. doi:10.1186/rr67

67. Plomgaard P, Nielsen AR, Fischer CP, et al. Associations between insulin resistance and TNF-alpha in plasma, skeletal muscle and adipose tissue in humans with and without type 2 diabetes. *Diabetologia*. 2007;50(12):2562-2571. doi:10.1007/s00125-007-0834-6

68. Matheny RW, Geddis AV, Abdalla MN, et al. AKT2 is the predominant AKT isoform expressed in human skeletal muscle. *Physiol Rep*. 2018;6(6):e13652. doi:10.14814/phy2.13652

69. Fielding RA, Gunstad J, Gustafson DR, et al. The paradox of overnutrition in aging and cognition. *Ann N Y Acad Sci*. 2013;1287:31-43. doi:10.1111/nyas.12138

70. Gumucio JP, Mendias CL. Atrogin-1, MuRF-1, and sarcopenia. *Endocrine*. 2013;43(1):12-21. doi:10.1007/s12020-012-9751-7

71. Carnac G, Vernus B, Bonnieu A. Myostatin in the Pathophysiology of Skeletal Muscle. *Curr Genomics*. 2007;8(7):415-422. doi:10.2174/138920207783591672

72. Salem M, Nath J, Rexroad CE, Killefer J, Yao J. Identification and molecular characterization of the rainbow trout calpains (Capn1 and Capn2): their expression in muscle wasting during starvation. *Comp Biochem Physiol B Biochem Mol Biol*. 2005;140(1):63-71. doi:10.1016/j.cbpc.2004.09.007